Clemson University
TigerPrints

All Theses | Theses

12-2006

ONLINE RESOURCES FOR LATE ADDITIONS TO THE SOLAR NEBULA

Allen Parker
Clemson University, pallen@clemson.edu

Follow this and additional works at: https://tigerprints.clemson.edu/all_theses

 Part of the Astrophysics and Astronomy Commons

Recommended Citation
Parker, Allen, "ONLINE RESOURCES FOR LATE ADDITIONS TO THE SOLAR NEBULA" (2006). *All Theses*. 41.
https://tigerprints.clemson.edu/all_theses/41

This Thesis is brought to you for free and open access by the Theses at TigerPrints. It has been accepted for inclusion in All Theses by an authorized administrator of TigerPrints. For more information, please contact kokeefe@clemson.edu.

ONLINE RESOURCES FOR LATE ADDITIONS TO THE SOLAR NEBULA

A Thesis
Presented to
the Graduate School of
Clemson University

In Partial Fulfillment
of the Requirements for the Degree
Master of Science
Physics

---

by
Allen L. Parker
December 2006

Accepted by:
Dr. Bradley S. Meyer, Committee Chair
Dr. Sean D. Brittain
Dr. Mark D. Leising

ABSTRACT

The presence of an excess of short-lived radionuclides in the early protoplanetary disk has been inferred from studying how the distribution of the abundances, in materials like Ca-Al-rich inclusions, differ from the solar abundance distribution (SAD). The likely source of these radioactivites is a supernova that ejected material into the early solar system. This thesis will discuss the solar abundance distribution and how a supernova may have contributed a 'late addition' of material into the early solar system. In addition, we have constructed online resources for studying these topics. This thesis will outline the Solar Abundance Tool, which allows a user to study the details of the solar abundance distribution, and the 1d Stellar Ejecta Module, which simulates a simplistic approach to the question of late additions.

DEDICATION

I dedicate my thesis to the loved ones who have helped me get this far.

Autumn,

I could not have done this without you. Whether in the form of a gummy bear basket or a hug, I know you are always thinking of me and it helps me keep going through the worst of it. Thanks for helping me with specifics of astronomy, listening to me rant about my problems, or even putting up with me gloating about regular expressions. As I step forward in life I know you will be there for me to offer your love and support to make sure I do not fall.

To my parents and sisters,

I owe who I am to you all. For raising me right, looking out for me, and always believing in me. I know you expect the best out of me, and I also know that you sincerely believe I am capable of the best. I can never thank you enough for the love and support you have given to me over the years.

ACKNOWLEDGEMENTS

I would like to acknowledge and personally thank all the members of the Webnucleo group who have helped me with my thesis and the research it describes. I thank Dr. Brad Meyer, my advisor, for his help guiding me through the largest concepts and the most minute details. I thank Dr. Jason Brown, for all of his technical support, and David Adams for his help with the Libnucnet Module.

I would also like to thank the members of my committee: Dr. Mark Leising and Dr. Sean Brittain, for their valuable time and input. And I would like to thank the NASA Cosmochemistry Grant for their support.

TABLE OF CONTENTS

Table of Contents (Continued)

List of Tables

LIST OF FIGURES

List of Figures (Continued)

CHAPTER 1
SOLAR ABUNDANCES

1.1 Introduction

The study of the Solar Abundance Distribution, SAD, is a complex area of research in the field of astrophysics today. The SAD refers to the abundances of all the various stable elements present in the Sun. Since the Sun contains about 98.86% of the solar system's mass [NASA 1991], the SAD is also representative of the abundances of stable elements in the entire solar system.

For the purposes of this thesis, I will review several aspects of the SAD: the basic motivation, a brief history, and several of the different techniques used to measure the SAD. In addition, I will discuss Webnucleo's Solar Abundances Tool and its relationship to the SAD in Chapter 3.

1.2 Motivation

Identifying the abundances of the elements in the Sun and our solar system is critical for many aspects of modern astrophysics. Our close proximity to the Sun gives astronomers many unique opportunities to study the abundances of the elements that are not available for any other star. Being able to infer the abundances of the elements from many different sources raises the accuracy of the SAD. This means we can use the Sun as a reference point from which to discuss the abundances of other stars.

One example that demonstrates how we use abundances to give us information about other stars is metallicity. The term metallicity may be used in a different ways, but a common definition by Carroll and Ostlie [1995] is:

$$\text{Metallicity} \equiv \left[\frac{Fe}{H}\right] \equiv \log\left(\frac{N_{Fe}}{N_H}\right) - \log\left(\frac{N_{Fe}}{N_H}\right)_{\odot} \tag{1.1}$$

Metallicity is one of the standard markers to help determine the age of a star. Stars are often characterized by their metalicity with respect to solar. Terms like metal-rich and metal-poor show this relationship.

Also, since the abundances are measured from different sources, such as meteorites and the photosphere, the composition and evolution of our solar system can be studied as well. For example, as discussed in Chapter 2, studying the difference between meteoritic and photospheric values leads astronomers to infer the presence of short-lived radioactivites in the early solar nebula. This inference contributes to solar system formation time scale models.

Understanding the SAD helps astronomers understand and develop solar or stellar atmospheric models as well as nucleosynthesis models. The observed abundances are important constraints on the output of the solar models.

1.3 History

Astronomers began cataloging some of the solar abundances as early as 1929, where the first such analysis was published by H.N. Russell [1929]. These observations, though without the assistance of modern technologies, allowed the astronomers of the time to make many conceptual leaps forward. His survey of 56 elements indicated a definite relationship between the mass number and the abundance of the elements. Heavier elements were significantly less abundant. Russell also found Hydrogen to be significantly more abundant than any other element.

Another pioneer of solar abundances was Unsöld, who published his findings in 1948. Unsöld [1948] was able to use more modern equipment and found, for the 25 elements he measured, that his results were similar to Russell's work 20 years prior.

Gldberg et al. [1960] established the first procedure to determine the solar abundances from photospheric data. The observed spectra are more precise and many parameters needed to infer the abundances are more accurate, but the techniques currently in use are similar[1] .

Today, there are various tables of abundances compiled by astronomers [Asplund et al. 2005; Anders and Grevesse 1989; Anders and Ebihara 1982; Grevesse and Sauval 1998; Lodders 2003]. These tables have combined results from all of the techniques developed.

---

[1] For more detail about the history of Solar Abundances, see the article by Lodders [2003].

The astronomical community is continually trying to improve the values and errors in the SAD.

1.4 Techniques

1.4.1 Photosphere

The first, and arguably the most prominent, technique to study the abundance of the elements in the Sun is spectroscopy of the photosphere. The procedure used to predict an element's abundance using photospheric information is complex. For example, there is a relationship between the equivalent width of an absorption feature and the number of atoms absorbing. This relationship is known as the curve of growth. Figure 1.1 is an example of such a curve. For a particular transition, a proper curve of growth can be measured or

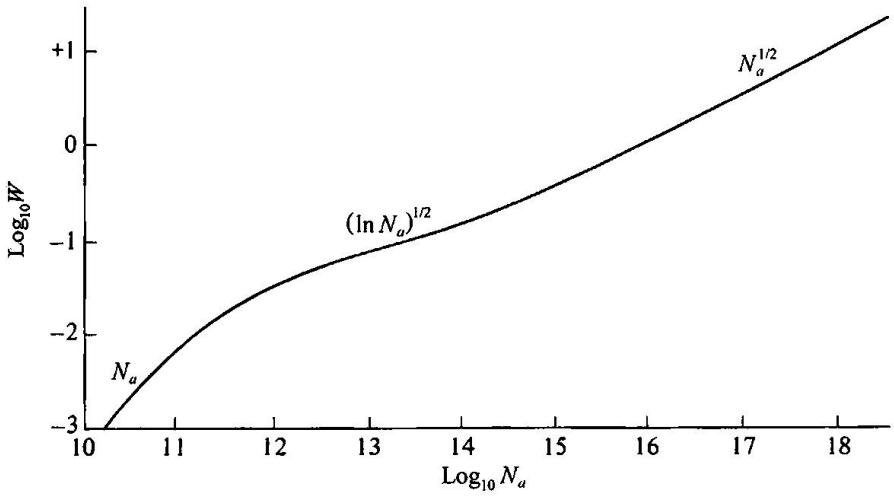

Figure 1.1 This is a curve of growth for the K line of Ca II [Carroll and Ostlie 1995, 301]. This is how the equivalent width of the atomic line changes with number of atoms absorbing.

theorized. With this curve, the the number of atoms of a particular element can be inferred.

Ideally, intensive spectroscopy could be done on the Sun's photosphere and characteristic atomic lines could be found for every element. However, there are many species

that are not observable in the Sun's photosphere. For example, one of the most abundant elements in the photosphere, ^{4}He cannot be directly observed. Instead ^{4}He can be predicted using stellar models, by helioseismological observations, or from solar wind observations. Also, photospheric abundances do not give much detailed information about the isotopic abundances of the elements. This is often because the features from less abundant isotopes are too small to be resolved from the line effects. Therefore, additional techniques are needed to complete the solar abundance picture.

1.4.2 Meteorites

Meteoritic Abundances are used frequently when determining the SAD. Many abundance studies are now done on Ivuna-type carbonaceous (CI) chondrites. CI chondrites show excellent agreement with the photospheric abundances and are thought to be representative of the early solar nebula. Because, CI chondrites condensed out of the early solar nebula material, they did not experience enough heating to melt and alter ther fine grain composition they are composed of. There have only been five such meteorites found so far, but they appear to to be excellent markers of the solar abundance distribution. The meteorites, and how they give us useful information, is discussed in greater depth in Appendix B.

1.4.3 Helioseismology

Since the Sun is optically thick, the measurements made from the photosphere only give information about the outer layers of the Sun. One technique developed to gain insight into the interior of the Sun is helioseismology. Helioseismology is the study of oscillations on the surface of the Sun. Studying how oscillations travel through and around the Sun gives astronomers information about the interior of the Sun in much the same way that earthquakes can be used to extrapolate the interior of the Earth.

Figure 1.2 gives a rough summary of the analysis steps that can be used when determining the abundances with helioseismology. First, the desired absorption line is isolated using filters. Then the intensities are measured using interferometers that can isolate a smaller range of frequencies. The change in intensity with time allows estimation of the Doppler shifts. With the Doppler shifts and the periods of oscillations, the velocities

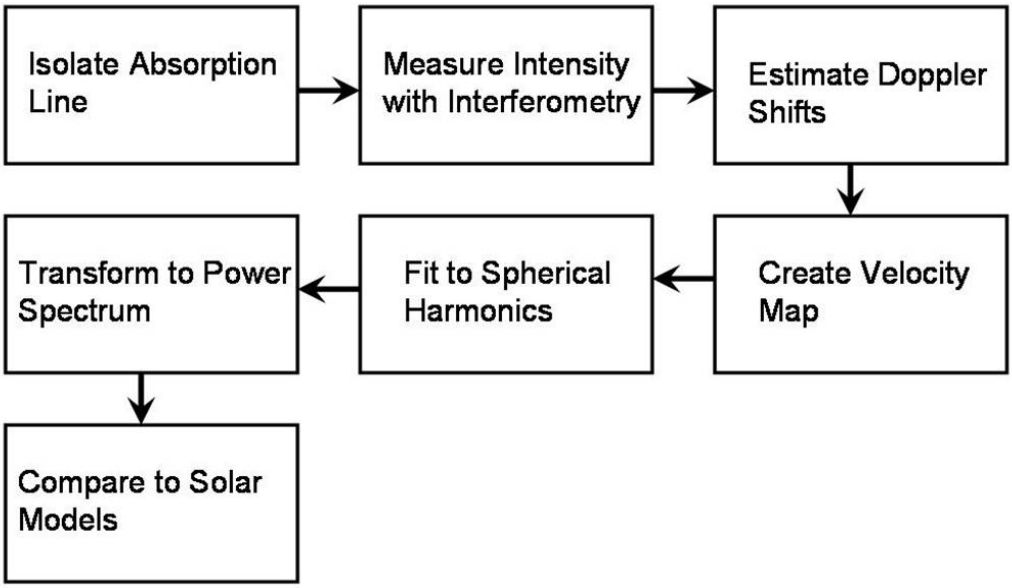

Figure 1.2 Qualitative flow chart to determine the abundances of the elements in the Sun using helioseismology.

and amplitudes on the surface are inferred. From the Dopplergrams, spherical harmonics are fit to the surface of the Sun. Then the time dependent coefficients of the spherical harmonics can be Fourier transformed to yield the velocities in terms of the oscillation frequencies. A power spectrum is then calculated (Figure 1.3). From this point, a model of the Sun or stellar atmosphere is needed to extract information about the interior. A model must include parameters such as: opacities, reaction rates, pressures, temperatures, and various other considerations. The goal is to fine tune the parameters to reproduce the observed surface oscillations.

One example of the kind of results one can obtain through helioseismic studies is to estimate the abundance of the helium in the solar envelope. Richard et al. [1998] determined that the mass fraction of helium in the solar envelope is 0.248 ± 0.002 using helioseismological techniques.

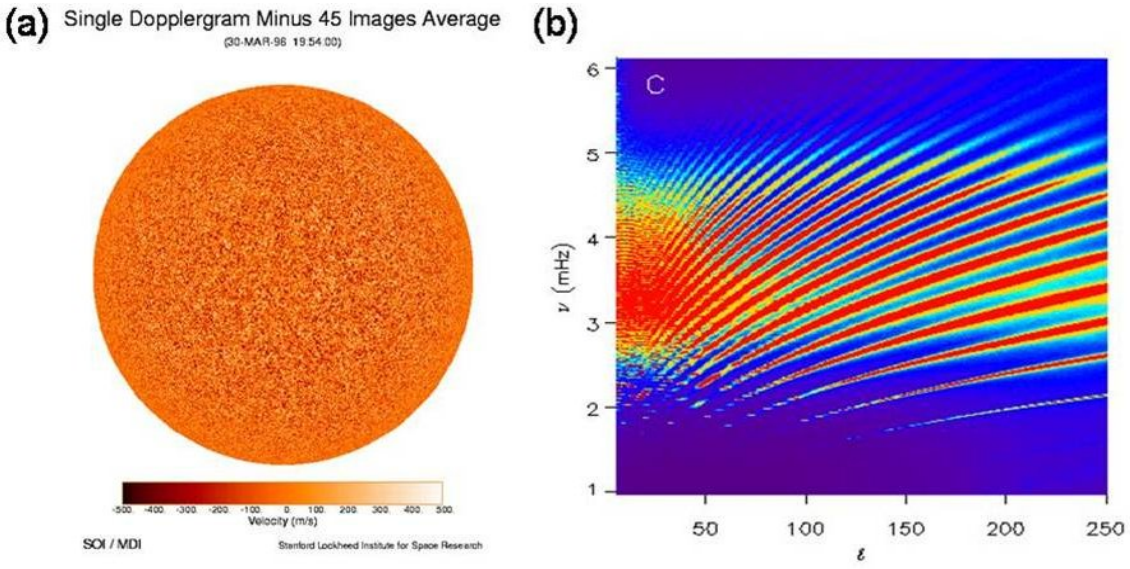

Figure 1.3 The left panel, (a), is an example of a Dopplergram from the Stanford Lockheed Institute for Space Research. The rotation of the Sun has been subtracted in order to see more clearly the local oscillations on the surface. The right panel, (b), is an example of an l-ν plot. This plot shows the relationship between the spherical harmonic order l and the observed frequency of oscillation. In addition, the color corresponds to the energy in that state. The bands of color trace constant value for the radial quantum number, n.

1.5 Numerical Systems

When discussing the SAD, there are two primary quantitative systems used: the cosmochemical and the logarithmic scales [Lodders 2003]. These provide a framework for comparison with abundance models for the Sun and other stellar systems. The cosmochemical scale makes each element a fraction of silicon, where the abundance of silicon is normalized to 10^6. This can be represented as:

$$N(El_i) = \left(\frac{\text{Number of atoms of element i}}{\text{Number of atoms of silicon}}\right) 10^6 \tag{1.2}$$

The logarithmic scale, by contrast, normalizes the abundance of hydrogen to 12. This definition of the abundance is represented:

$$A(El_i) = \log\left(\frac{\text{Number of atoms of element i}}{\text{Number of atoms of hydrogen}}\right) + 12 \tag{1.3}$$

For a sense of scale, Table 1.1 has several common elements and the value of their abundance in both systems.

Element	$N(El_i)$	$A(El_i)$
Hydrogen	2.79×10^{10}	12.00
Helium	2.72×10^{9}	10.99
Carbon	1.01×10^{7}	8.56
Silver	4.86×10^{-1}	1.24
Uranium	8.99×10^{-3}	-0.49

Table 1.1 A comparison of the abundance of several different elements in the cosmochemical scale and the logarithmic scale.

CHAPTER 2
LATE ADDITIONS TO THE SOLAR NEBULA

There is evidence that, in the early solar nebular many short-lived radioactivities were present in abundances not characteristic of the steady state equilibrium. These species are inferred from abundance measurements made on meteorites found today. In CAIs (Calcium-Aluminum rich Inclusions, see Appendix B), we can look for an overabundance in the 'daughter' nuclide of a radioactive species. By referencing this overabundance with other stable isotopes, the abundance of the short-lived radioactive nuclide when the inclusion was formed can be deduced.

Many of the radioactive nuclides are difficult or impossible to form in events characteristic of the early solar system. This means that, in order to find species like ^{60}Fe, an external source is needed. One mechanism is that material from a supernova could have been injected into the solar system in the early stages of formation. Some go further to discuss how this late injection from a supernova may have even triggered the collapse of the solar cloud itself [Cameron and Truran 1977].

In this chapter, I will discuss in more detail how these abundances are inferred and a simple treatment of the injection process.

2.1 Inference of Short-Lived Radioactivities

Since the radioactive species we are interested in are long extinct, we must use measurements made today to derive how much of a radioactive nuclide must have been present in the early solar nebula. An example of this deduction is ^{26}Al.

^{26}Al decays into ^{26}Mg with a half life of approximately 0.72 Myr. Since the ^{26}Al has fully decayed, the ^{26}Mg observed today is a combination of what was initially present and the ^{26}Al that was present [Podosek 2005].

$$^{26}\mathrm{Mg}_{\mathrm{Today}} = ^{26}\mathrm{Mg}_{\mathrm{Initial}} + ^{26}\mathrm{Al}_{\mathrm{Initial}} \tag{2.1}$$

Then, Equation 2.1 is normalized with respect to a stable isotope of magnesium that has not changed from the formation of the CAI to the time of measurement. In the case of magnesium, ^{24}Mg is used.

$$\left(\frac{^{26}\mathrm{Mg}}{^{24}\mathrm{Mg}}\right)_{\mathrm{Today}} = \left(\frac{^{26}\mathrm{Mg}}{^{24}\mathrm{Mg}}\right)_{\mathrm{Initial}} + \left(\frac{^{26}\mathrm{Al}}{^{24}\mathrm{Mg}}\right)_{\mathrm{Initial}} \tag{2.2}$$

To complete this relationship, we also express ^{26}Al in terms of its stable isotope reference, ^{27}Al.

$$\left(\frac{^{26}\mathrm{Mg}}{^{24}\mathrm{Mg}}\right)_{\mathrm{Today}} = \left(\frac{^{26}\mathrm{Mg}}{^{24}\mathrm{Mg}}\right)_{\mathrm{Initial}} + \left(\frac{^{26}\mathrm{Al}}{^{27}\mathrm{Al}}\right)_{\mathrm{Initial}} \left(\frac{^{27}\mathrm{Al}}{^{24}\mathrm{Mg}}\right)_{\mathrm{Today}} \tag{2.3}$$

Now, the unknown initial quantities are expressed in a linear relationship of the measured values. This means that the slope of a graph made by plotting ^{27}Al/^{24}Mg on the x axis and ^{26}Mg/^{24}Mg on the y axis will yield a slope of ^{26}Al/^{27}Al. These types of plots are called isochrons. So, given several measurements we can infer how much ^{26}Al with respect to ^{27}Al must have been present when the CAI formed.

2.2 Approximate Treatment

The basic idea behind the late injection is that material from a nearby supernova mixed with the early solar nebula. In this section I will discuss a very simple way to treat this problem and how it may be improved.

Stars can be broken up in to various zones using the Lagrangian mass coordinate. Each zone is a shell of mass that will have a different distribution of the nuclides therein. (See Appendix A for a further discussion of mass zones.) This gives a one dimensional picture of a star where the abundance distribution only depends on a radial coordinate. When a star goes supernova it undergoes explosive nucleosynthesis and ejects its outer layers into the ISM (inter-stellar medium).

A reasonable first approximation is to take the outer layers from a supernova and consider this the material to be ejected. Then, take this material and inject it into the solar nebula. For now, the depth of the zones ejected may be considered a free parameter. This is because there are many physical reasons that might change what shells escape to

the solar nebula. For example, the extent of supernova fallback, or the loss to Wolf-Rayet stellar winds may change the zones ejected [Meyer and Clayton 2000]. The injection mass cut, or zones ejected, can be narrowed by observing what radionuclides we need to find in the solar nebula. For example, for a $21M_{\odot}$ star, the mass cut must be at least as deep as $7.5M_{\odot}$ in order for ejecta to include any of the radionuclides besides ^{26}Al [Meyer 2005]. This reduces the parameter space of the mass cut that needs to be explored numerically.

A cloud of material created in this way will have both stable isotopes and many short-lived radioactive species formed from the nuclear burning and explosive supernova nucleosynthesis. The material is then free to decay for some time interval, t.

Species	$\tau_{1/2}$ (Myrs)
^{26}Al	0.72
^{36}Cl	0.3
^{41}Ca	0.1
^{53}Mn	3.7
^{60}Fe	1.5
^{107}Pd	6.5
^{129}I	16
^{146}Sm	103
^{182}Hf	9

Table 2.1 The half-lives of nine short-lived radionuclides [Meyer 2005].

To isolate the time for the decay, several species of interest and their respective decay rates are listed in Table 2.1. Notice the half life of ^{26}Al, ^{36}Cl, and ^{41}Ca are all less than one million years. This means the decay time, t, must be on the order of megayears or shorter to retain enough radioactive material to match the abundances inferred from the isochrons discussed above. Further, since some of these radioactive species, like ^{36}Cl, are created with such a large overabundance in a star, a few half-lives are needed to lower the ^{36}Cl abundances to levels suggested by experiment. This means that, in order to explain the measured anomolies in CAIs, decay times that seem most probable are close to one or two megayears.

Since the CAI forming mechanism has not been settled upon, is not clear where the ejecta from the supernova spends most of its time before condensing. However, given a particular model of formation, further limitations may be placed on the decay time giving more information about how the solar system formed. Thus, within certain limits, t will still be considered a free parameter in this approximation as well.

Finally, the decayed material will mix with the solar nebula. Here the ratio of mixing must be considered as the CAIs are forming. In a sense, this is the third free parameter to this first order treatment of the stellar injection phenomenon. This single ratio can be thought of as a combination of two different components of the mixing. (Mixing ratios are discussed further in Appendix C.) The first component relates the absolute mass of the material to be injected to the mass of the solar nebula. In other words, since our solar system formed from about $1M_{\odot}$ of material from the early solar nebula, how much supernova ejecta material, per solar mass, was injected? The second component refers to the homogeneity of the mixing. The easiest approximation is to assume the material mixes homogeneously before any CAIs are formed.

I have discussed to three major free parameters in this simple mixing model: the injection mass cut, the time of decay, and the mixing ratio. In order to recreate some of the anomalies measured in today's CAIs, these parameters must be chosen. Work has been done by B. S. Meyer [2000] showing that, for a decay interval of one million years and a mass cut of about $4M_{\odot}$, an injection ratio on the order of $10^{-4}M_{\odot}$ is required in order to recreate the inferred (^{26}Al/^{27}Al) value.

The discussion above is clearly an overly simplistic view of what actually occurs. However, it does establish a framework from which to identify specific areas to improve the approximation. For example, so far, we have assumed the ejecta from the supernova is one dimensional in nature, and is mixed homogeneously. In reality, the various layers of material are not clearly defined and will mix in complex ways. This means the material from different zones may not be equally weighted. One way to approach this problem is to run simulations of supernovae that include the full complexities of relativistic hydrodynamics in order to determine how the ejecta might be comprised. Another approach is to leave the relative weights of the zones as variable. In this way it may be possible to determine what

kind of mixture would be necessary to explain the short-lived radioactivities by working backwards.

CHAPTER 3

SOLAR ABUNDANCES ONLINE TOOL

Webnucleo's Solar Abundances Online Tool is a more interactive way to view and understand the SAD. Users can view, sort, and plot the abundances in various ways. While the default abundances are those of Anders and Grevesse [1989], users can choose any SAD data to upload to the tool. In this chapter I will give examples of how to use the tool[1] .

Here I will cover the various features of the tool and how to use it with the default values. At this point it may be helpful to launch the Solar Abundances Tool available at: http://nucleo.ces.clemson.edu/online_tools/solar_abundances/0.1 .

After launching the tool, the first panel you will see is the 'Upload Table' panel. This panel will load a table of solar abundances from an XML file you provide or a set of default values.

Begin by clicking the 'Use Default Abundances' button in the 'Upload Table' panel as shown in Figure 3.1. When the table has successfully loaded, you should see a screen like the one in Figure 3.2. Click next to proceed.

Figure 3.1 This screenshot is of the 'Upload Table' panel. By clicking 'Use Default Abundances' the abundances by Anders and Grevesse [1989] are loaded.

[1] For more information on the details of the Solar Abundances Tool see Appendix E.

Figure 3.2 This screenshot shows what the Solar Abundances Tool should look like after the default abundances have been successfully loaded.

The next panel is the 'Sort Data' Panel. This panel has been designed to help sort all of the solar abundance data. Here, you may choose to sort the data by atomic number (Z), mass number (A), neutron number (N), or by abundance. Also, you may choose ascending or descending order in order to find the information most relevant for you. For this tutorial select 'Z' in the 'Sort by' drop down menu and select the 'Ascending' radio button as shown in Figure 3.3. Click 'View Abundance Table' to proceed. The Abundance Table will appear in a new window (Figure 3.4). To explore some of the other features of this tool, return to the Solar Abundances Tool and click 'Next'.

Figure 3.3 This screenshot is of the 'Sort Data' panel where the options have been selected to sort the abundances by ascending order in the atomic number, Z.

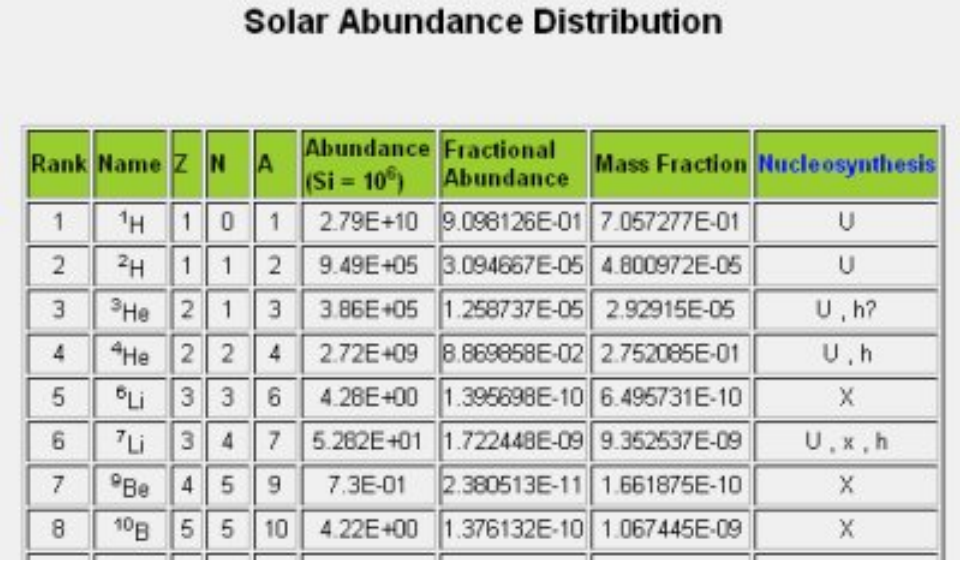

Solar Abundance Distribution

Rank	Name	Z	N	A	Abundance (Si = 10^6)	Fractional Abundance	Mass Fraction	Nucleosynthesis
1	^{1}H	1	0	1	2.79E+10	9.098126E-01	7.057277E-01	U
2	^{2}H	1	1	2	9.49E+05	3.094667E-05	4.800972E-05	U
3	^{3}He	2	1	3	3.86E+05	1.258737E-05	2.92915E-05	U , h?
4	^{4}He	2	2	4	2.72E+09	8.869858E-02	2.752085E-01	U , h
5	^{6}Li	3	3	6	4.28E+00	1.395698E-10	6.495731E-10	X
6	^{7}Li	3	4	7	5.282E+01	1.722448E-09	9.352537E-09	U , x , h
7	^{9}Be	4	5	9	7.3E-01	2.380513E-11	1.661875E-10	X
8	^{10}B	5	5	10	4.22E+00	1.376132E-10	1.067445E-09	X

Figure 3.4 This is a screenshot of the abundances sorted by ascending order in Z.

The 'Plot Abundances' Panel allows you to view a plot of the solar abundances grouped together by either Z, A, or N. This means that all nuclides that share the same atomic number (Z), for example, will be summed and plotted as one data point. For this tutorial, select 'Z' from the 'plot on x-axis' drop down menu and select 'Logarithmic' from the 'y-axis type' drop down. Now, click 'View Plot' as shown in Figure 3.5. This will yield a plot like Figure 3.6.

In the window that comes up there is a 'View Data' button that will bring up another window that has all the data points that are contained in the plot. Return to the Solar Abundances Tool and click 'Next' to proceed to the next panel.

The 'Table Abundances' will create a table that contains all the grouped abundances. Select each of the available elements as shown in Figure 3.7 and click 'View HTML Table' or 'View ASCII Table'. The HTML table will look like Figure 3.8. An ASCII table will look like Figure 3.9. Return to the Solar Abundances Tool and click 'Next' to access the next feature.

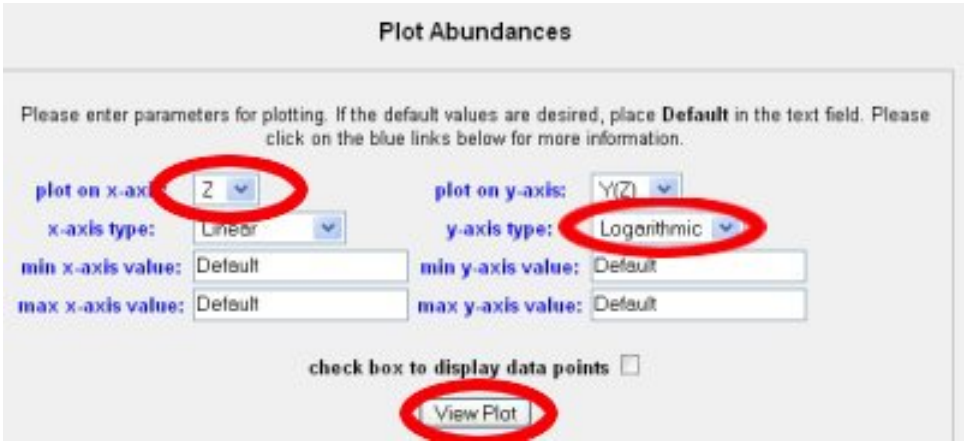

Figure 3.5 This screenshot of the 'Plot Abundances' panel shows the correct selections to create a plot with the Atomic Number, Z, on the x-axis, the Abundances on the y-axis. Selecting 'Logarithmic' under the 'y-axis type' drop down menu will make the data easier to see.

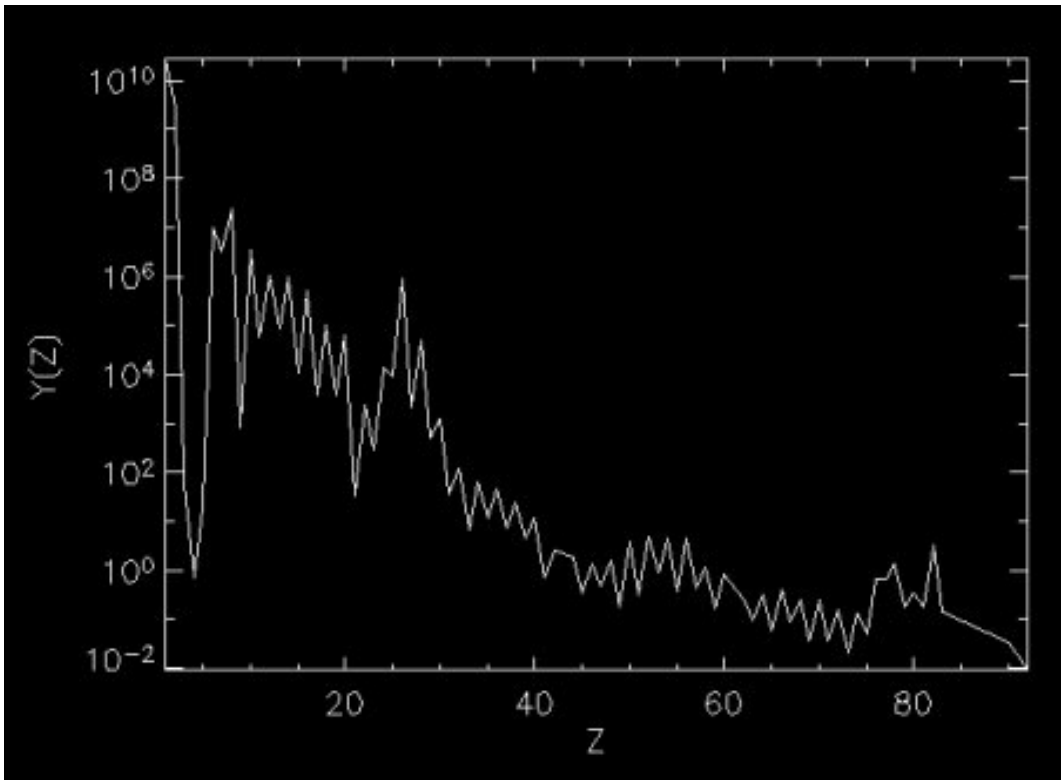

Figure 3.6 This plot of Y(Z) versus Z was generated by the Solar Abundances Tool using the default data.

Figure 3.7 This screenshot selects all elements on the 'Table Abundances' panel in order to display them together in a table.

Index	Y(Z)	Y(A)	Y(N)
0	0.0000000	0.0000000	2.7900000e+10
1	2.7900949e+10	2.7900000e+10	1335000.0
2	2.7203860e+09	949000.00	2.7200000e+09
3	57.100000	386000.00	4.2800000
4	0.73000000	2.7200000e+09	52.820000
5	21.200000	0.0000000	4.9500000
6	10101000.	4.2800000	9990017.0
7	3131500.0	52.820000	3231000.0
8	23756640.	0.0000000	23711500.

Figure 3.8 This screenshot shows the format of an HTML table generated with the Solar Abundances Tool.

```
Index   Y(Z)   Y(A)   Y(N)
0  0.0000000  0.0000000  2.7900000e+10
1  2.7900949e+10  2.7900000e+10  1335000.0
2  2.7203860e+09  949000.00  2.7200000e+09
3  57.100000  386000.00  4.2800000
4  0.73000000  2.7200000e+09  52.820000
5  21.200000  0.0000000  4.9500000
6  10101000.  4.2800000  9990017.0
7  3131500.0  52.820000  3231000.0
8  23756640.  0.0000000  23711500.
```

Figure 3.9 This screenshot shows what an ASCII table generated with the Solar Abundances Tool will look like.

The ‘Plot All’ panel will generate plots using the data from each individual nuclide. The example we will use in this tutorial is to plot Abundance versus mass number (A). To do this, select ‘A’ from the ‘plot on x-axis’ and ‘Abundance’ from the ‘plot on y-axis’. In addition, select ‘Logarithmic’ from the ‘y-axis type’. Check the box marked ‘check box to display data points’. This will make a second checkbox appear, ‘check box to turn off line connections’; and check it also as shown in Figure 3.10. After all these settings have been changed, click ‘View Plot’ to create a Plot like Figure 3.11.

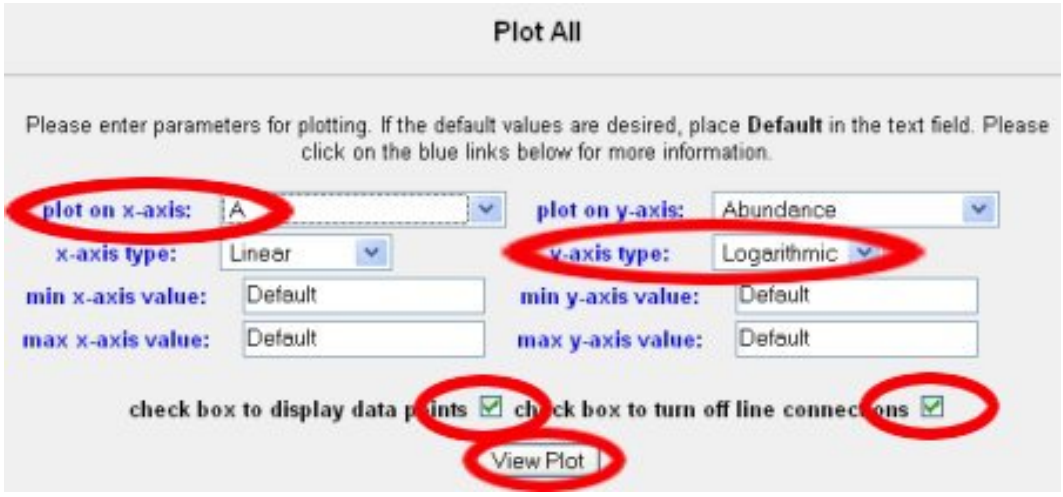

Figure 3.10 This screenshot shows the recommended settings for generating a plot of the abundances versus the mass number, A.

The ‘Full Table’ panel will generate a table with all the data for the individual nuclides. Check all the boxes and click the ‘View HTML Table’ or ‘View ASCII Table’ as shown in Figure 3.12. Like the ‘Abundances Table’ panel, these buttons will generate the tables. Click either ‘View HTML Table’ or ‘View ASCII Table’.

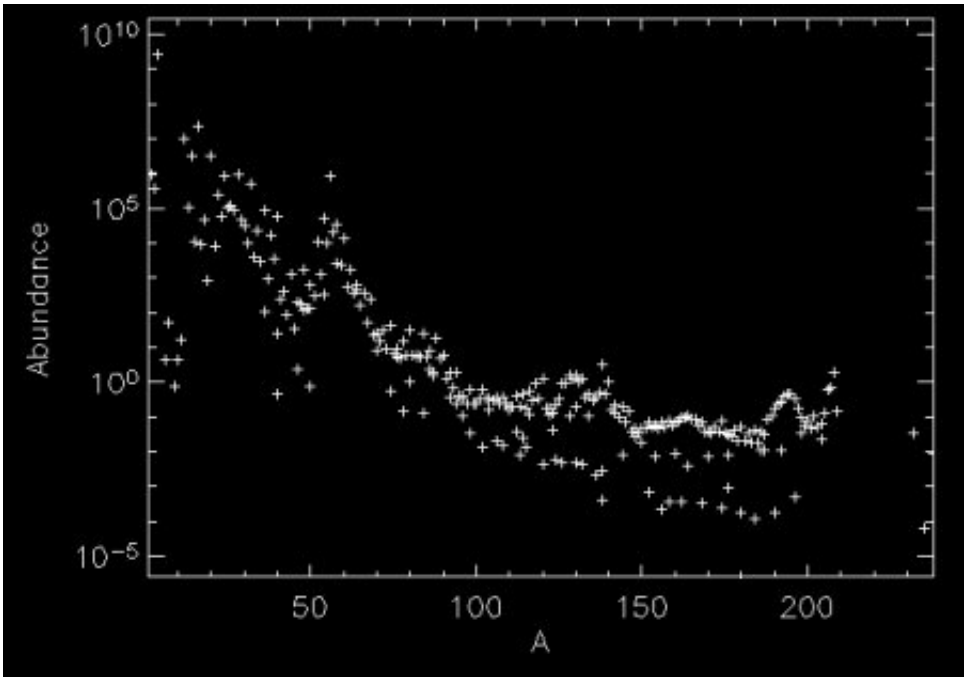

Figure 3.11 This plot, generated by the Solar Abundances Tool, has Abundance on the y-axis and the atomic number on the x-axis. Notice, since this is the 'Plot All' panel, there may be more than one data point for a given atomic number.

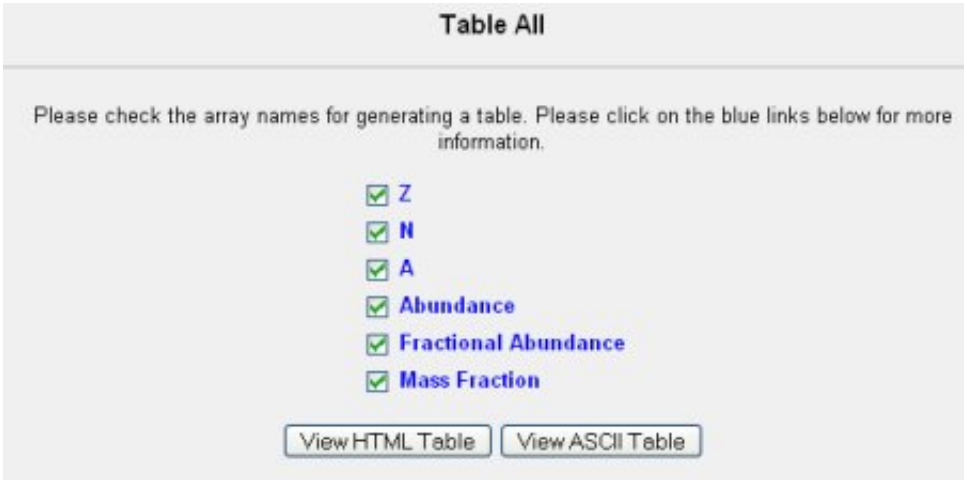

Figure 3.12 This screenshot shows the various elements that can be written to an HTML or ASCII table from the 'Full Table' panel. Like the 'Plot All' panel, the abundances written to the table are for the individual nuclides. They are not grouped by common atomic numbers like in the first table panel (Figure 3.7).

CHAPTER 4
STELLAR EJECTA ONLINE MODULE

To simulate the late addition of material to the solar nebula, Webnucleo has developed a 1d Stellar Ejecta Module. This module takes the outer layers from a star, decays them through time, and mixes them with the solar abundance distribution. To use this tool, download the distribution available at:
http://nucleo.ces.clemson.edu/home/modules/wn_1d_stellar_ejecta/ .

In this chapter I'll discuss the format of the input files needed to use the wn_1d_stellar_ejecta module, the routines used to simulate the process, and the output of the each of the routines.

4.1 Input Data

The wn_1d_stellar_ejecta module requires two different forms of input. The first is an HDF5 file (Appendix D.3) containing the abundances of various species in the supernova material by zone. The second is an XML file (Appendix D.1) containing the material the ejecta is to be mixed with.

The zones in the HDF5 file refer to spherical shells of material and are characterized by the amount of the star's mass within the shells inner radius. This mass unit can be thought of as a radial coordinate within the star and is represented in the HDF5 file as the 'M_r' dataset in the 'Star' group (Figure 4.1).

The species contained in the star are identified by the Z and A datasets within the 'Species' group. Each element within the Z dataset should be thought of as coupled with the element in the A dataset that shares the same index. Each element of the Z and A dataset is an integer.

Also within the 'Star' group is a two dimensional dataset of double precision floating point numbers labeled 'Abundances'. This dataset contains the abundances as a function of the species and the zones. The columns are the various zones within the star and are coupled with the value of M_r for the same index number. The species are along the rows and are coupled with the elements of the same index from the Z and A datasets. In this

way there must be as many rows to 'Abundances' as there are elements of Z and A, and as many columns as there are elements in 'M_r'.

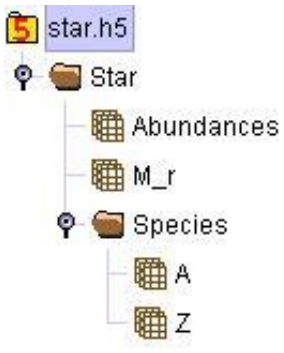

Figure 4.1 This Figure is a screenshot of the input HDF5 file for the wn_1d_stellar_ejecta module as seen in HDFview. The file contains all of the abundances of the star's species as a function M_r.

The other input data needed is an XML file with the solar abundance distribution. This XML file must contain a series of z, a, and abundance tags. For an example of a properly formated XML file, download the distrubition of the Solar Abundances Tool (Chapter 3).

4.2 Routines

This module uses routines written in both C and IDL (Appendix D.2) and reads files from HDF5 (Appendix D.3) and XML (Appendix D.1) files. The basic computational pipeline is represented in Figure 4.2. In this section, I will discuss each routine in more depth.

4.2.1 wn1dstellarejecta__createDecayXml

The first IDL routine, wn1dstellarejecta__createDecayXml, reads the HDF5 input file, mixes the outer zones desired, and writes the renormalized abundances to an XML file. This means the various zones chosen are grouped together as a single group. The group of nuclides are treated as being homogeneously mixed.

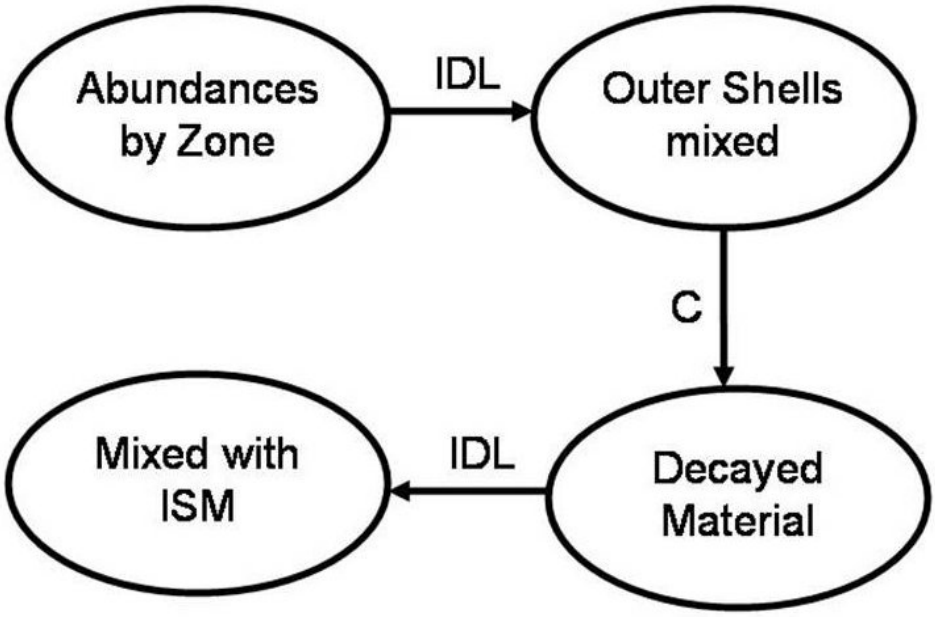

Figure 4.2 The overall flow to the module is shown here. The data is read in and the outer are mixed together using routines written in IDL. The nuclear decay is performed in C, and the decayed material is mixed into the ISM using an IDL routine.

The syntax for this routine is:

```
wn1dstellarejecta__createDecayXml, 'input.h5', 'output.xml', mr_limit
```

Here, input.h5 is the HDF5 file described earlier, output.xml, is the resulting XML file produced, and mr_limit is the value of M_r for the inner most zone of the supernova to be included in the outer layers.

4.2.2 wn1dstellarejecta__combine.xsl

The next step is to add other information to the XML file, such as the decay rates. To accomplish this an XSLT stylesheet is used (Appendix D.1.2). This stylesheet copies the mass fractions written by wn1dstellarejecta__createDecayXml and the nuclear data information from wn1dstellarejecta__NuclearData.xml and combines them to one XML file. The syntax for this step is:

```
xsltproc --stringparam decayed.xml wn1dstellarejecta__combine.xsl
  doc2.xml > output.xml
```

The XML generated at this step is now ready to be used in the decay process. To ensure this XML file is of the correct format it, it can be checked with the XSD schema, Libnucnet__schema.xsd.

It is worth noting that the steps described until now do not need to performed each time before running the decay routine. Once you have a well formed XML file that adheres to the Libnucnet__schema.xsd schema, that XML file can be modified directly. However, the user will be responsible for preserving the features of the XML file. For example, the initial mass fractions must sum to unity. This means if one would like to add a small initial mass fraction to one nuclide, it must be balanced by a modification to a second nuclide. Otherwise, the user may have to renormalize all the mass fractions themselves. A renormalization script, or XSLT stylesheet, would not be difficult to write, but as of yet, is not a feature in the wn_1d_stellar_ejecta module.

4.2.3 wn1dstellarejecta__decay

The material in the combined XML then evolves in time and undergoes weak decays using the routine, wn1dstellarejecta__decay that calls Webnucleo's Libnucnet Module[1] .

The weak_decay routine writes out an HDF5 file with the information for each time step of the decay. The structure of this HDF5 file is shown in Figure 4.3.

The HDF5 file has the species listed in a table where the atomic numbers, mass numbers, and element names are all listed. The 'Abundances' dataset is a two dimensional set of doubles. The column number corresponds to a particular time step and the row number corresponds to a particular nuclide. The parameters table contains t, the time step, and dt, the time increment.

---

[1] For a complete description of the routines in Libnucnet see David Adam's Master's thesis [2006] or its online documentation available at:
http://nucleo.ces.clemson.edu/home/modules/libnucnet/ .

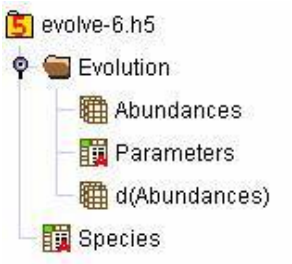

Figure 4.3 The HDF5 format for the output is given here. The abundances for all nuclides present in the ejecta are recorded for each time step in the decay.

4.2.4 wn1dstellarejecta__mix

Once the decay is completed the ejected material can be mixed with the ISM by using the IDL routine, wn1dstellarejecta__mix. This routine lets the user weight the ratio of the ejecta's mass and the mass of the other abundance distribution. The syntax for the mixing routine is:

```
wn1dstellarejecta__mix, 'ism.hdf5',  'decayed.xml', mass_ratio
```

This routine returns a structure to IDL so the user may immediately begin interacting with the output. In order to write out the result of the mixing to a file, three procedures are available in order to ensure a user can have the output in the most convenient format. These procedures are: wn1dstellarejecta__writeMixedAscii, wn1dstellarejecta__writeMixedHdf5, and
wn1dstellarejecta__writeMixedXml. The only parameter that is passed to these procedures is the structure generated from the mixing.

APPENDICES

Appendix A

Nuclear Burning

For the Stellar Ejecta module, one provides the data from a stellar model he or she would like to use as the ejecta. For example, this data can be generated by creating a star of the desired mass out of solar type material and evolving it through its life. For a massive star (M>10$M_{\odot}$) the star burns through Si and undergoes further nucleosynthesis as it goes supernova. In this section I will discuss the main stages of burning[1] .

The basic sequence of the burning stages goes: hydrogen, helium, carbon, neon[2] , oxygen, and finally silicon. This discussion will shed light onto some of the features seen in the plots of the stellar data and the solar abundances used throughout this thesis.

A.1 Hydrogen Burning

Once hydrogen burning begins in a star it is considered to be on the main sequence. This stage is responsible for taking the lighter element ^{1}H and creating ^{4}He. The reaction chain is referred to as the CNO bi-cycle and is shown in Figure A.1.

In this sequence of reactions there are several noteworthy aspects. First is that, for the cycle that begins and ends with ^{12}C, also known as the CN cycle, the net reaction is:

$$4p \rightarrow^{4} \mathrm{He} + 2\nu + 2e^{+} + 3\gamma \tag{A.1}$$

However, since the proton capture of ^{14}N into ^{15}O is slow compared to the other reactions, an overabundance of ^{14}N builds up during the hydrogen burning stage. As the ^{14}N builds up the species that initiate the cycle, ^{12}C, is depleted. For the cycle that begins and ends with ^{14}N, also known as the ON cycle, the net reaction is also given by Equation A.1. In this cycle, the proton capture of and subsequent breakup of ^{17}O into ^{14}N and ^{4}He is comparatively slow, so there is a build up of ^{17}O during the hydrogen burning stage. Similar to ^{12}C, ^{16}O is the first unique species to the ON cycle, and is depleted as ^{14}N is built up.

---

[1] For further information on supernova nucleosynthesis and the main burning stages see the review paper by Meyer [1997] or the text by Arnett [1996].

[2] since this stage does not stop the star from contracting it is often not considered a true burning stage

$$
\begin{aligned}
{}^{12}\mathrm{C} + \mathrm{p} &\rightarrow {}^{13}\mathrm{N} + \gamma \\
{}^{13}\mathrm{N} &\rightarrow {}^{13}\mathrm{C} + e^{+} + \nu \\
{}^{13}\mathrm{C} + \mathrm{p} &\rightarrow {}^{14}\mathrm{N} + \gamma \\
{}^{14}\mathrm{N} + \mathrm{p} &\rightarrow {}^{15} + \gamma \\
{}^{15}\mathrm{O} &\rightarrow {}^{15}\mathrm{N} + e^{+} + \nu
\end{aligned}
$$

$$
{}^{15}\mathrm{N} + \mathrm{p} \rightarrow {}^{12}\mathrm{C} + {}^{4}\mathrm{He}
\qquad
\begin{aligned}
{}^{15}\mathrm{N} + \mathrm{p} &\rightarrow {}^{16}\mathrm{O} + \gamma \\
{}^{16}\mathrm{O} + \mathrm{p} &\rightarrow {}^{17}\mathrm{F} + \gamma \\
{}^{17}\mathrm{F} &\rightarrow {}^{17}\mathrm{O} + e^{+} + \nu \\
{}^{17}\mathrm{O} + \mathrm{p} &\rightarrow {}^{14}\mathrm{N} + {}^{4}\mathrm{He}
\end{aligned}
$$

Figure A.1 This figure shows the reaction chains involved in the CNO bi-cycle. Once ^{15}N is produced the chain branches into two possibilities. The dominant cycle is the branch to the left where the net reaction converts 4 ^{1}H into 1 ^{4}He, 2 positrons, and 2 electron neutrinos.

The overall result of the CNO cycle is that the ^{1}H is consumed and an overabundance of ^{4}He, ^{14}N, and ^{17}O is created while ^{12}C and ^{16}O are depleted.

A.2 Helium Burning

Once the star has used up the available supply of hydrogen in the core where the temperature is hot enough for the CNO cycle to occur, the balance between the nuclear radiation pressure and the gravitation pressure is lost. This means the star will begin to collapse. As the star compresses the temperatures will increase. The core will soon be hot enough to ignite the helium burning reaction chains. This helium burning core will be smaller in extent than the hydrogen burning core was. Also, the burning of the helium will create a shell, where the hydrogen is not fully depleted, hot enough to ignite hydrogen burning again. This means that, even after the helium burning stage, there will be a shell that has the characteristic overabundances as described in the hydrogen burning section.

Helium burning involves the fusing of ^{4}He atoms together. However, the product of two ^{4}He atoms, an excited ^{8}Be atom, is highly unstable and does not live long enough to have an appreciable abundance. This fact of the nuclear burning process explains the

dearth of elements of atomic number 8 in the solar abundance distribution seen in the Solar Abundances Tool (Figure 3.6). Beryllium is essentially skipped in in the nuclear reactions a star undergoes.

^{8}Be can sometimes survive long enough to capture another ^{4}He which results in the more stable ^{12}C atom. The overall reaction is thus:

$$^{4}\mathrm{He} + ^{4}\mathrm{He} + ^{4}\mathrm{He} \rightarrow ^{12}\mathrm{C} \tag{A.2}$$

^{12}C can also capture another ^{4}He resulting in ^{16}O.

The production of ^{16}O and ^{12}C are the direct result of the fusing of helium, but at the temperatures helium burning occurs, other reactions may take place to create further products. From the hydrogen burning there was a build up of ^{14}N due to the slow conversion of ^{14}N to ^{15}O. This free ^{14}N can now capture a ^{4}He atom and initiate the following sequence of reactions:

$$\begin{aligned}
^{14}\mathrm{N} + ^{4}\mathrm{He} &\rightarrow ^{18}\mathrm{F} + \gamma \\
^{18}\mathrm{F} &\rightarrow ^{18}\mathrm{O} + e^{+} + \nu \\
^{18}\mathrm{O} + ^{4}\mathrm{He} &\rightarrow ^{22}\mathrm{Ne} + \gamma \\
^{22}\mathrm{Ne} + ^{4}\mathrm{He} &\rightarrow ^{25}\mathrm{Mg} + \mathrm{n}
\end{aligned}$$

In this way, the overabundance of ^{14}N from hydrogen burning is yields a new source of ^{18}O and ^{22}Ne. It is also worth noting that, due to the low temperatures during helium burning (relative to later stages), the final reaction creating ^{25}Mg from ^{22}Ne is small compared to the creation of ^{22}Ne. However, this reaction does create enough neutrons to begin enriching the heavier elements into their more neutron rich isotopes.

By the end of the helium burning stage an overabundance of ^{12}C, ^{16}O, ^{18}O, and ^{22}Ne is created at the expense of ^{4}He and ^{14}N. In addition, neutron rich isotopes are created during helium burning and will exhibit overabundances as well.

A.3 Carbon Burning

With the helium depleted in the core, the star contracts again until the temperatures are hot enough to ignite carbon burning. Like before, the region of the carbon burning core

is smaller than the helium burning core or the hydrogen burning core that proceeded it. From the helium burning, there is an overabundance of ^{12}C when carbon burning begins. Two ^{12}C atoms combine to form one atom of ^{24}Mg. This ^{24}Mg atom is in an excited state and will quickly make a transition to one of several possibilities as shown in Figure A.2. During this stage an excess of protons and neutrons are available to capture onto other

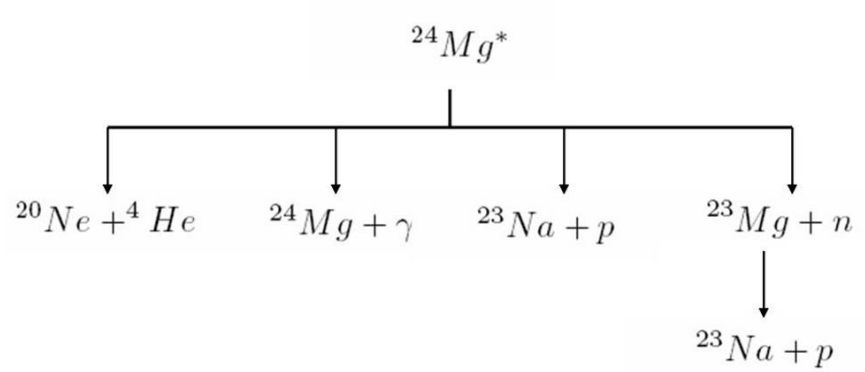

Figure A.2 The possible transitions available to the excited ^{24}Mg atom.

elements. Much like the free neutrons described in the helium burning section, this allows many secondary products to be made during the carbon burning. The main products of this phase are ^{24}Mg, ^{20}Ne, and ^{23}Na. These are produced at the expense of the carbon burned.

A.4 Neon Burning

As the carbon fuel dwindles, the star begins to contract again. During this contracting the core will become hot enough to initiate a short period of neon burning. This stage does not stop the collapse of the star, however, so neon is burned as the star collapses.

The ^{20}Ne in the core undergoes two different processes. First, a ^{20}Ne atom can break apart into ^{16}O and ^{4}He.

$$^{20}\text{Ne} + \gamma \rightarrow ^{16}\text{O} + ^4\text{He} \tag{A.3}$$

With ^{4}He available for capture, ^{20}Ne can also become ^{24}Mg.

$$^{20}\mathrm{Ne} + ^{4}\mathrm{He} \rightarrow ^{24}\mathrm{Mg} + \gamma \tag{A.4}$$

Thus, this brief burning phase enhances the reservoir of ^{16}O that began in the helium burning phase and also adds to the overabundance of ^{24}Mg began during the carbon burning.

A.5 Oxygen Burning

The star now contracts until temperatures are sufficient to fuse the overabundance of oxygen created during the helium and neon burning phases. Here, two ^{16}O are fused directly to an excited state of ^{32}S.

$$^{16}\mathrm{O} + ^{16}\mathrm{O} \rightarrow ^{32}\mathrm{S}^{*} + \gamma \tag{A.5}$$

The excited state of ^{32}S created here will quickly break apart into one of many possible outcomes as shown in Figure A.3.

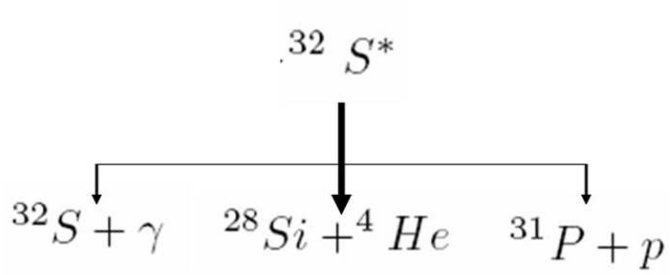

Figure A.3 The possible transitions the unstable ^{32}S* can make. The most likely result is that the atom will breaks apart into ^{28}Si and ^{4}He.

Since the ^{32}S* usually forms ^{28}Si, it is the main product of oxygen burning. However, there are free protons and ^{4}He released and any number of secondary isotopes may be formed by the capture of these.

A.6 Silicon Burning

The star undergoes one final contraction that will initiate silicon burning. Similar to neon burning, rather than fusing two ^{28}Si atoms directly together, silicon breaks apart into lighter elements. The breakup of ^{28}Si frees ^{4}He atoms that can combine with heavier atoms.

At the temperatures required for silicon burning, ^{4}He atoms can combine with the heavier elements, but will also disintegrate off of them at comparable rates. This means an equilibrium is reached between the various elements where capturing and releasing ^{4}He particles occurs.

I will not develop this equilibrium further here, but for a further discussion regarding the Quasi-Static Equilibrium (QSE), Nuclear Statistical Equilibrium (NSE), and how it results in a supernova, see the work by Meyer [1997].

A.7 Discussion

I have discussed the major burning stages of a massive star ($>10M_{\odot}$) and the major products formed throughout. Since our Sun is still in its hydrogen burning phase, hydrogen and helium are the most abundant, but because the initial make up of our solar system came from stars that have undergone the reactions described above, many features from the burning phases are seen in the solar abundance distribution. While a complex variety of other products are made by the capturing of protons, neutrons or helium atoms during the later burning stages and the supernova itself, following the main products will help us interpret some of the more prominent features of the solar abundance distribution.

Figure A.4 contains two plots made directly from the Solar Abundances Tool (Chapter 3). Here we can see a feature that demonstrates a property of the nuclear reactions described in the early burning stages. Notice there is a sharp drop in abundance at from Z=3 to Z=5 and from A=6 to A=11. Recall that the main product of the hydrogen burning is ^{4}He and the main product of the helium burning is ^{12}C. Some of the elements between ^{4}He and ^{12}C may be created through other secondary processes but they are not produced in any of the primary reactions. The elements in between are effectively skipped by the primary reactions.

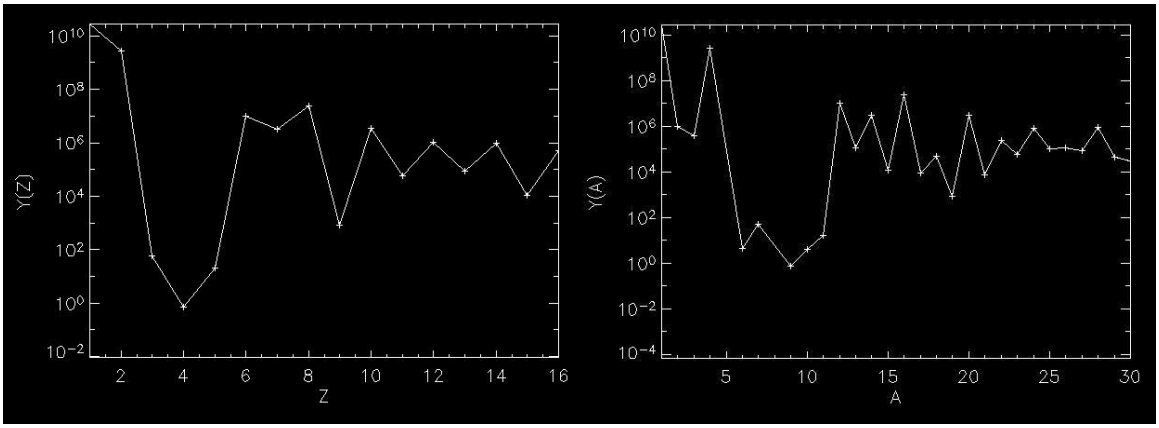

Figure A.4 This figure, made from the Solar Abundances Tool, shows many of features that reflect the burning stages discussed in this section.

There is another sharp drop at Z=9, or Fluorine, and a corresponding dip from A=17 to A=19. Again, this is because the main products of the burning stages jump from ^{16}O to ^{20}Ne.

Even at heavier elements there is still an oscillation in Z that that peaks for even values of Z. This represents nuclei being formed in multiples of ^{4}He. Likewise the abundances as a function of A oscillate. Multiples of four are the most abundant species.

This discussion should serve to show how the features seen in abundance plots, such as the solar abundance distribution, are not just statistical variations, but representative of the nuclear processes that occur in stars and eventually enrich the ISM.

Appendix B

Chondrites

At various points in this thesis I have discussed abundance measurements made on different components of meteorites. For example, many solar abundance measurements are taken from CI (I-type carbonaceous) chondrites and many isotopic anomalies measured in CAIs (Calcium-Aluminum rich Inclusions) are used to discuss what short-lived radionuclides were present in the early formation of the solar system. In this appendix, I will discuss further what these meteoritic components are and how they yield this scientific information.

B.1 Basic Composition

A general Chondrites has a few basic features. They are composite particles that are typical composed of three main components: chondrules, refractory inclusions, and matrix material. Since chondrites are composite particles, their size tends to be on the order of centimeters. This is in contrast to many of the components within a chondrite that are generally on the order of millimeters. For example, the average diameter of chondrules measured is about 0.5mm.

What is very important about chondrites is that upon collecting the components mentioned above, they are not heated to the point where they will melt and mix the components together. This means that the history of the individual components are preserved.

Chondrites are further classified into different types: carbonceous, ordinary, enstatite, and other. The carbonceous chondrites are considered the most primitive (characteristic of the early solar nebula). They are characterized by the presence of water and/or minerals showing alterations from water and large amounts of carbon. Enstatite chondrites show evidence of heating but not to temperatures sufficient to melt the meteorite. Enstatites are characterized by the form the iron takes. The iron is typically found in iron sulfide or with nickel in a metallic form [Darling 2006]. Ordinary chondrites are the most frequently found chondrites and typically have a very small percentage of refractory inclusions. Ordinary chondrites have experienced some heating but not as much as the enstatite group and so are less altered. The final category, other, consists of chondrites with metal percentages that are significantly different from the first three types. For example, K-type

Other chondrites have an unusually high percentage of iron, while R-type Other chondrites are unusually depleted in metals such as iron and nickel.

For the purposes of this thesis, I will focus on CI chondrites because they are frequently used in determining the solar abundances and CAIs because they are a primary source of data when discussing the late additions of short-lived radioactivites to the solar nebula[3] .

B.2 CI Chondrites

The CI chondrites are thought to be the most primitive of the chondrites because about ninety-five percent of their composition is the fine grained matrix characteristic of the early solar nebula. The 'I' comes from Ivuna, the first chondrite to be included in this category. To date there have only been five Ivuna type carbonaceous chondrites.

The CI chondrites, being composed primarily of the matrix material, show the closest agreement to the photospheric measurements (with exceptions for H, He, C, N, O, and the noble gases). This relationship is shown in Figure B.1 quite well.

B.3 Ca-Al-rich Inclusions

One of the components found in many chondrites are Calcium-Aluminum rich Inclusions. These inclusions are typically on the order of several millimeters and occasionally up to a centimeter. This is in contrast to many of the components within a chondrite that are generally on the order of millimeters. For example, the average diameter of chondrules measured is about 0.5mm.

As the name would imply, they have been enriched in minerals like calcium, aluminum, and often titanium as well. CAIs form from events that heat protoplanetary disk material to 1400K or greater. This is known because the CAIs have minerals that are stable at these temperatures. For example, CAIs often formed with: spinel ($MgAl_2O_4$), melitite , Ca-Ti-pyroxene, and anorthite ($CaAl_2Si_2O_8$).

From $^{207}Pb/^{206}Pb$ dating CAIs are thought to be the earliest solids to form in the solar system. Figure B.2 shows an example of a lead-lead plot. Since ^{235}U decays into ^{207}Pb

---

[3] For a further review on the chondritic meteorites see [Scott and Krot 2005].

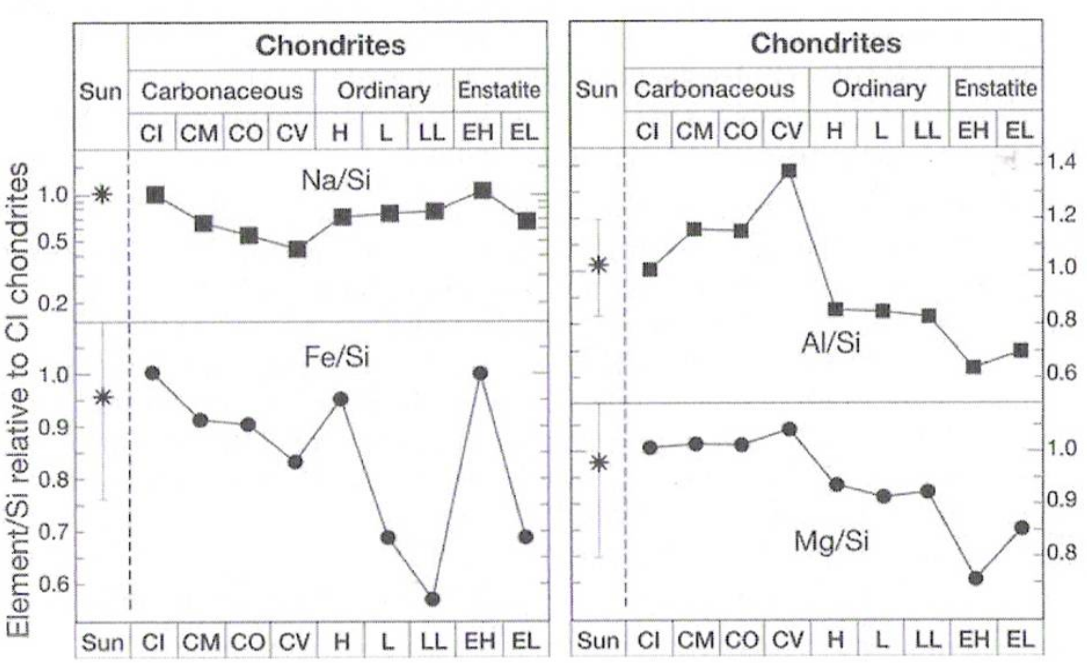

Figure B.1 This figure shows how the different forms of chondrites relate to the solar abundance values for several specific species [Scott and Krot 2005].

and ^{238}U decays into ^{206}Pb, the difference in these time scales can be used to determine how old a sample must be. In these studies, all meteorites measured are presumed to have the same initial ^{207}Pb/^{204}Pb and ^{206}Pb/^{204}Pb ratios. This means that all elements that share the same age will fall along a line in a plot of ^{207}Pb/^{204}Pb versus ^{206}Pb^{204}Pb. Current lead-lead dating techniques indicate that CAIs are about 4.56 Gyrs old. This means they are likely formed in the early stages of the protoplanetry disk.

Upon heating and condensing, a snap-shot of the material at that time is formed. Then, it is possible to use abundance measurements of CAIs to track the radioactivites present in the early solar system.

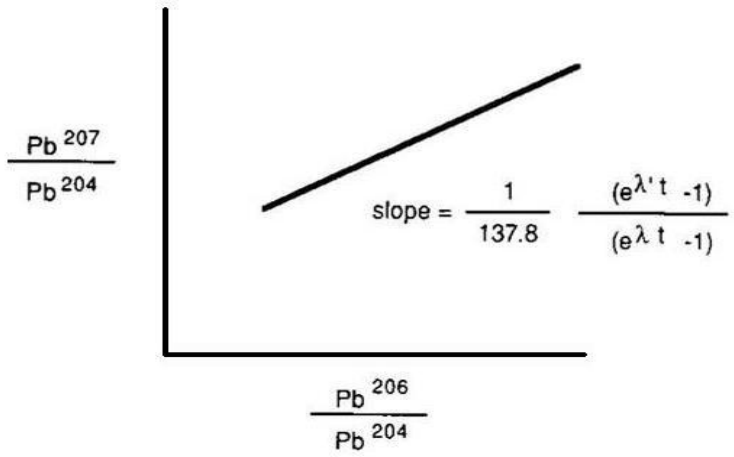

Figure B.2 This figure shows how a lead-lead isochron can yield the age of CAIs [Kerridge and Matthews 1988]. All CAIs that share the same age will fall along a particular line. Then, using the equation for the slope here, the age can be determined. Here, λ' is the decay constant for ^{235}U into ^{207}Pb and λ is the decay constant for ^{238}U into ^{206}Pb.

Appendix C

Three-Isotope Plots

The mixing in the Stellar Ejecta Module does not necessarily have to be homogeneous. In this appendix, I will discuss mixing the reservoirs inhomogeneously and how a three-isotope plot may help visualize this mixing. To develop how this may help, I will discuss how the mass fractions of the species being mixed vary linearly with a mixing coefficient.

C.1 Linearity by Example

For a homogeneous mixture, the mass fraction of a particular species, x_i, can be represented by Equation C.1 where R is given by Equation C.2. Here, $x_i^{(1)}$, represents the mass fraction of species i in the first reservoir, and $x_i^{(2)}$ in the second. This will be denoted as the bulk mixture.

$$x_i^{\text{bulk}} = x_i^{(1)} R + x_i^{(2)}(1 - R) \tag{C.1}$$

$$R = \frac{M_{\text{total}}^{(1)}}{M_{\text{total}}^{(1)} + M_{\text{total}}^{(2)}} \tag{C.2}$$

In order to create a mixture different than the bulk mixture, the mass of the reservoirs can be varied. This mixing ratio, f, is given by Equation C.3 and the resulting mixed sample is given by Equation C.4.

$$f = \frac{M_{\text{sample}}^{(1)}}{M_{\text{sample}}^{(1)} + M_{\text{sample}}^{(2)}} \tag{C.3}$$

$$x_i^{\text{sample}} = x_i^{(1)} f + x_i^{(2)}(1 - f) \tag{C.4}$$

To illustrate what these different definitions mean for the resulting mass fraction of species i, I will use the example values in table C.1 and plots generated in IDL (Appendix D.2).

First, Equation C.4 depends linearly on f. This means for the values in Table C.1, a simple linear plot can be generated (as shown in Figure C.1). Further, plots generated comparing two species will be linear as well. This relationship is shown in Figure C.2.

Variable	Value
$x_i^{(1)}$	0.75
$x_i^{(2)}$	0.25
$x_j^{(1)}$	0.3
$x_j^{(2)}$	0.6
$x_k^{(1)}$	0.1
$x_k^{(2)}$	0.7
R	0.2
x_i^{bulk}	0.35
x_j^{bulk}	0.54

Table C.1 This table contains numerical values for the constants used when generating the IDL figures in this section.

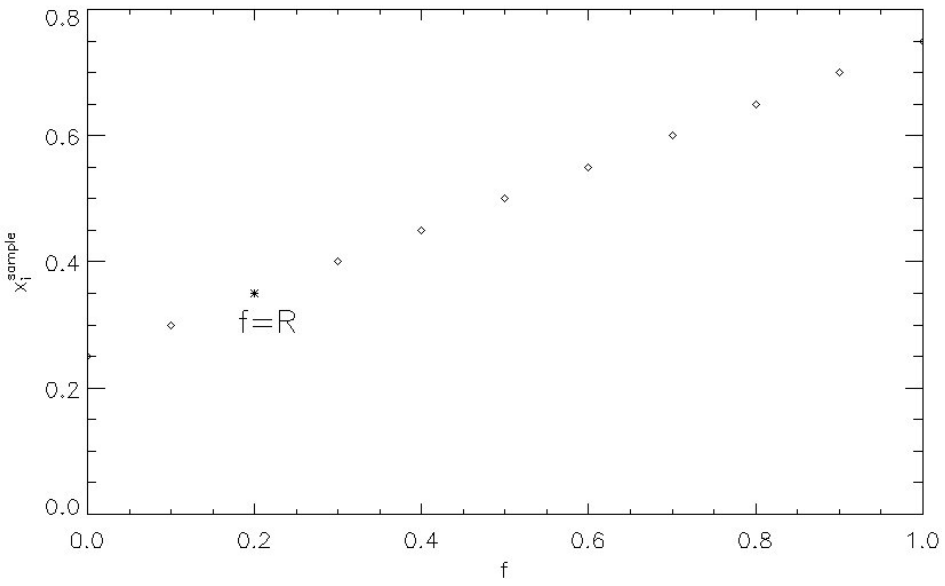

Figure C.1 This figure shows the linear relation ship between a sample, expressed by Equation C.4, and the mixing factor, f, is linear. Notice that the homogeneous case, when f is equal to R, is labeled in this figure and denoted by an asterisk. Here, the end points of the graph correspond to the mass fractions from the initial reservoirs.

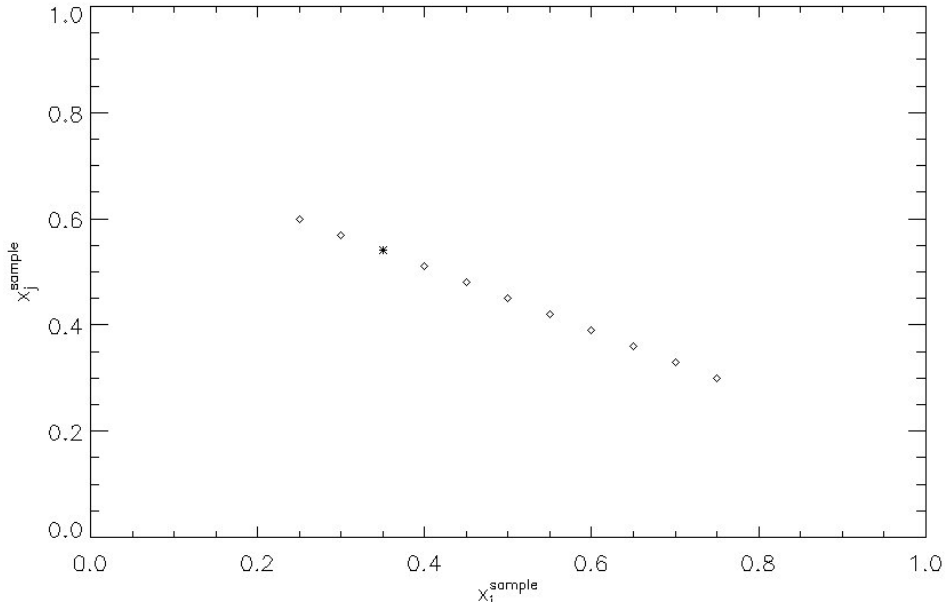

Figure C.2 This figure shows that, as a function of f, two independent species will vary linearly with respect to each other. The homogeneous case is denoted with an asterisks and the end points are once again the values of the initial reservoirs.

Rathr than discussing absolute abundances, astronomers instead use relative abundances to make comparisons. As such, we often look at the relationship of three separate species as a method of normalization. For example, when studying the short-lived radionuclides discussed in Chapter 2, we need to talk about the abundance of a radioactive species with respect to a stable isotope. In other words, the more appropriate measurement from a sample may be $(x_i/x_k)^{\text{sample}}$. Then, to compare two species with respect to a common reference, we plot $(x_j/x_k)^{\text{sample}}$ versus $(x_i/x_k)^{\text{sample}}$, as shown in Figure C.3. While this plot still yields a linear relationship, it is stretched by the third species. The stretching is only as strong as the difference of x_k in the different reservoirs. So, if $x_k^{(1)}$ equals $x_k^{(2)}$ the plot will resemble Figure C.2, only scaled by a constant.

It is conventional to renormalize the mass fractions such that the origin represents the standard, or homogeneous, case [Faure 1986]. Also, since the typical deviations from

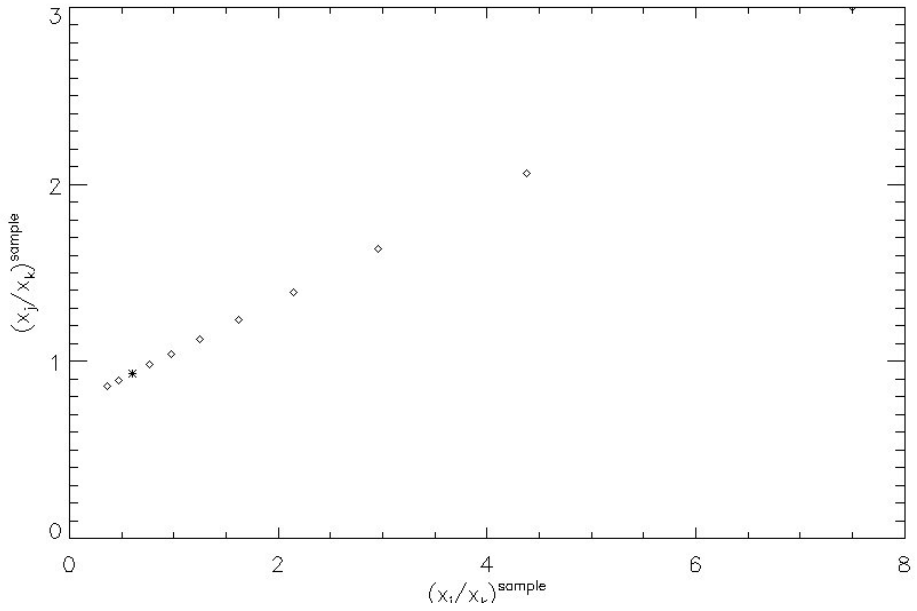

Figure C.3 This figure shows the relationship between two species when referenced to a third species that will vary with the mixing coefficient as well. Again, there is a linear relationship and the homogeneous case is denoted by an asterisk. However, notice that the data points stretch apart. This is a result of the third isotope also varying linearly with f. In the case where $x_k^{(1)}$ is equal to $x_k^{(2)}$, the graph will not be stretched and it will more closely resemble Figure C.2.

homogeneity will be small, a scaling factor of 1000 is used. This transformation is given by Equation C.5 and the example is shown in Figure C.4.

$$\delta x_i = \left[\frac{\left({}^{x_i}/_{x_k} \right)_{\text{sample}}}{\left({}^{x_j}/_{x_k} \right)_{\text{bulk}}} - 1 \right] \times 1000 \tag{C.5}$$

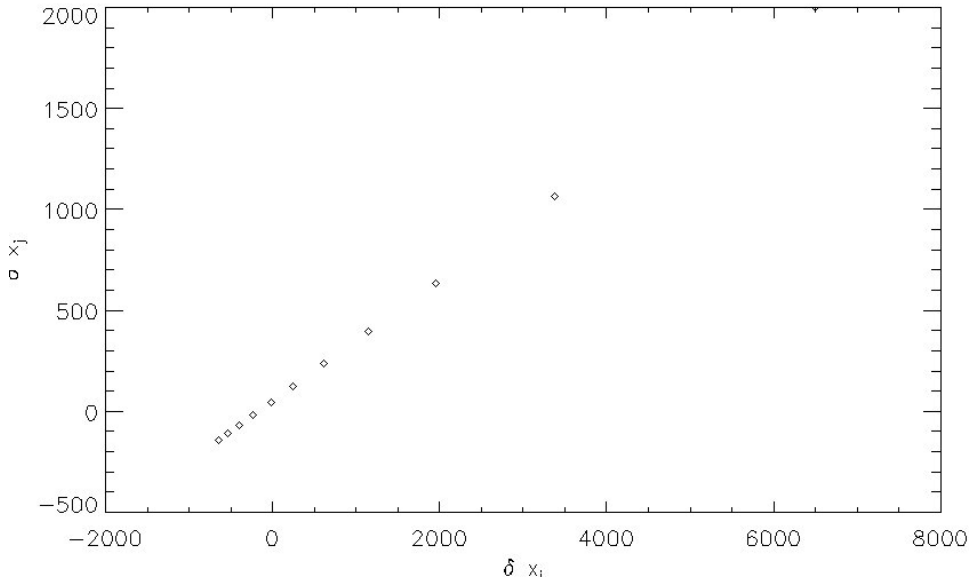

Figure C.4 This 'delta-delta' plot, shows the same relationship between the parameters as Figure C.3, but the origin now represents the case of homogeneous mixing and the deviations from homogeneity are scaled by a factor of 1000. Again, the end points correspond to the δ values of the individual reservoirs.

C.2 Linearity Developed Analytically

To generalize these examples, these relationships can be shown analytically as well. The linearity between an individual isotope and f is trivially shown by Equation C.6.

$$x_i^{\text{sample}} = \left(x_i^{(1)} - x_i^{(2)} \right) f + x_i^{(2)} \tag{C.6}$$

To show the linearity of the two-isotope plot, solve Equation C.6 for f.

$$f = \frac{x_i^{\text{sample}} - x_i^{(2)}}{x_i^{(1)} - x_i^{(2)}} \tag{C.7}$$

Inserting this form of f into an expression for x_j^{sample} in the form of Equation C.6 yields the following.

$$x_j^{\text{sample}} = \left(x_j^{(1)} - x_j^{(2)}\right)\left(\frac{x_i^{\text{sample}} - x_i^{(2)}}{x_i^{(1)} - x_i^{(2)}}\right) + x_j^{(2)} \tag{C.8}$$

Rewriting this shows the linear relationship between x_j^{sample} and x_i^{sample}.

$$\begin{gathered} x_j^{\text{sample}} = \left(\frac{x_j^{(1)} - x_j^{(2)}}{x_i^{(1)} - x_i^{(2)}}\right) x_i^{\text{sample}} + \left(\frac{x_i^{(2)}\left(x_j^{(2)} - x_j^{(1)}\right)}{x_i^{(1)} - x_i^{(2)}} + x_j^{(2)}\right) \\ x_j^{\text{sample}} = \mathrm{C}_1 x_i^{\text{sample}} + \mathrm{C}_2 \end{gathered} \tag{C.9}$$

Finally, to see the linear relationship in the three-isotope plot, notice that since x_i^{sample} and x_j^{sample} can be written in terms of f and various constants (D_l), δx_i and δx_j can be written as the following (where the factor of 1000 has been dropped for convenience).

$$\begin{aligned} \delta x_i &= \left(\frac{\mathrm{D}_1 f + \mathrm{D}_2}{\mathrm{D}_5 f + \mathrm{D}_6} - 1\right) \\ \delta x_j &= \left(\frac{\mathrm{D}_3 f + \mathrm{D}_4}{\mathrm{D}_5 f + \mathrm{D}_6} - 1\right) \end{aligned} \tag{C.10}$$

Both expressions can be solved for f and then set equal to each other to yield Equation C.11.

$$\frac{\mathrm{D}_2 - (1 + \delta x_i)\,\mathrm{D}_6}{\mathrm{D}_5\,(1 + \delta x_i) - \mathrm{D}_1} = \frac{\mathrm{D}_4 - (1 + \delta x_j)\,\mathrm{D}_6}{\mathrm{D}_5\,(1 + \delta x_j) - \mathrm{D}_3} \tag{C.11}$$

When cross-multiplied, the result is Equation C.12.

$$\begin{aligned} &\mathrm{D}_2\mathrm{D}_5\,(1 + \delta x_j) + \mathrm{D}_3\mathrm{D}_6\,(1 + \delta x_i) - \mathrm{D}_2\mathrm{D}_3 - \mathrm{D}_6\mathrm{D}_5\,(1 + \delta x_i)\,(1 + \delta x_j) \\ &\qquad = \mathrm{D}_4\mathrm{D}_5\,(1 + \delta x_j) + \mathrm{D}_1\mathrm{D}_6\,(1 + \delta x_i) - \mathrm{D}_4\mathrm{D}_1 - \mathrm{D}_6\mathrm{D}_5\,(1 + \delta x_i)\,(1 + \delta x_j) \end{aligned} \tag{C.12}$$

The terms that are quadratic in the δ variables cancel out and we are left with only linear terms in the δ variables and constants. This means we are left with the effective form shown in Equation C.13.

$$\delta x_j = \mathrm{D}_7 \delta x_i + \mathrm{D}_8 \tag{C.13}$$

By carrying all of the constants, it can be shown that the slope of a delta-delta plot (D_7) is given by Equation C.14.

$$D_7 = \frac{\left(x_j^{(1)} x_k^{(2)} - x_k^{(1)} x_j^{(2)}\right)}{\left(x_i^{(1)} x_k^{(2)} - x_k^{(1)} x_i^{(2)}\right)} \tag{C.14}$$

C.3 Application to Late Additions

This appendix has discussed how various species relate to one another when mixing reservoirs to varying degrees of homogeneity. This can be of use when studying the late additions to the solar nebula discussed in this thesis. The assumption that a homogeneous cloud of material is ejected into a homogeneous abundance distribution and then mixes homogeneously, is an idealized scenario used to help develop an understanding of the injection process. A somewhat less restrictive assumption would be to assume that the homogeneous components are free to mix with varying ratios. This means, in terms used above in sections C.1 and C.2, the material to be injected can be expressed as $x_i^{(1)}$, and the early solar nebula as $x_j^{(2)}$. These separate reservoirs may be mixed anywhere from f=0 to f=1, in principle. This new freedom will allow the idea of a late injection to explain CAIs that exhibit varying abundances in the short-lived radioactive species. In other words, by considering different values of f, one injection of material into the early solar system can produce a continuum of possible mixtures. Since the material that condenses into a particular CAI may not have been homogeneously mixed before condensing, we may expect to see any number of possible mixtures experimentally.

As mentioned earlier, the end points of a three-isotope plots are the values of the individual reservoirs. In our case, the mass fractions of the solar nebula are significantly better understood than the injected material. Thus, we may treat the end point corresponding to solar as fixed. If this treatment is a fair approximation for the physical mechanism, experimental delta-delta plots will yield a relatively linear relationship. Somewhere along that line would be the correct value for the homogeneous mixture, and from that we could infer the bulk makeup of the injected material.

Studying delta-delta plots like this may not conclusively yield the composition of the injected material, but it does limit the parameter space that must be explored theoretically or computationally. Understanding the linear relationships produced in these graphs, in conjunction with the material, by zone, from a supernova and the decay rates of the radioactive species, may help us understand the source of the overabundance of short-lived radioactivities in the early solar system.

Appendix D

Technical Resources

D.1 XML: Extensible Markup Language

In the development of our tools XML, Extensible Markup Language, is used frequently. Utilizing XML enables us to structure large sets of data in an organized and human readable format. In addition, XML is the basis for much of the standards backed by the W3C (World Wide Web Consortium).

A basic XML file contains 'tags' and 'attributes' that organize data into a hierarchy of information. In this way, XML can be used as a way to database information.

Arguably the most important feature of XML is that it is easily readable independent of computer background. For simple tables of data the advantages of XML may not be apparent, but consider a more complex set of data like the minutes of a meeting. Figure D.1 is an example of how to organize that data.

D.1.1 XSD: XML Schema Definitions

Much of the power of XML lies in the ability to write XML Schema Definition, XSD, files and Extensible Stylesheet Language Transformations, XSLT, files. XSD files make it easy to check the structure and content of an XML file quickly. For the example in Figure D.1 an XSD can be written to quickly check whether or not all the necessary information for a particular meeting has been entered. Figure D.2 shows what an XSD file might look for for the example here.

D.1.2 XSLT: Extensible Stylesheet Language Transformations

XSLT files allow us to style any the data in any XML file that adheres to a particular schema. This means the style information can be separate from the way the data is organized in the XML file. For the example developed in Figures D.1 and D.2, we may want to write a stylesheet to show all the item titles, but without displaying the presenter's name or the synopsis. A basic XSLT file that would accomplish this is shown in Figure D.3. This example shows several powerful features available in XSLT. For example, the 'value-of' command extracts the content of a particular tag to be displayed in the finished styled file.

```
<minutes>
  <meeting>
    <date>20061017</date>
    <item>
       <presenter>Allen Parker</presenter>
       <title>Importance of XML</title>
       <synopsis>XML is a convenient way to organize data.</synopsis>
    </item>
    <item>
       <presenter>John Doe</presenter>
       <title>Importance of W3 Standards</title>
    </item>
  </meeting>
  <meeting>
    <date>20061103</date>
    <item>
       <presenter>Tom Smith</presenter>
       <title>Tom's Title</title>
    </item>
    <item>
       <presenter>Bob Edwards</presenter>
       <title>Bob's Title</title>
    </item>
  </meeting>
</minutes>
```

Figure D.1 Example of a basic XML file. Minutes are divided into separate, individual meetings. Each meeting is further sub-divided into presenter, title, and synopsis. The hierarchical format is convenient to keep track of nested information and is easy for any user to read and understand.

```
<?xml version="1.0" encoding="ISO-8859-1" ?>
<xsd:schema
  xmlns:xsd="http://www.w3.org/2001/XMLSchema"
>
  <xsd:element name="minutes" type="minutes_type" />

  <xsd:complexType name="minutes_type" >
    <xsd:sequence>
      <xsd:element name="meeting" type="meeting_type"
        minOccurs="1"
      />
    </xsd:sequence>
  </xsd:complexType>

  <xsd:complexType name="meeting_type">
    <xsd:sequence>
      <xsd:element name="date" type="xsd:integer"
        minOccurs="1" maxOccurs="1"
      />
      <xsd:element name="item" type="item_type"
        minOccurs="1" maxOccurs="10"
      />
    </xsd:sequence>
  </xsd:complexType>

  <xsd:complexType name="item_type">
    <xsd:sequence>
      <xsd:element name="presenter" type="xsd:string" />
      <xsd:element name="title"  type="xsd:string" />
      <xsd:element name="synopsis" type="xsd:string"
        minOccurs="0" maxOccurs="1"
      />
    </xsd:sequence>
  </xsd:complexType>

</xsd:schema>
```

Figure D.2 This XSD will check the format of the XML example in Figure D.1. It checks each individual element to make sure its contents of the 'string' datatype. Also, it checks to make specifies the minimum and maximum occurrences of many of the elements. For example, there can only be one date specified for a particular meeting, but the the synopsis element is optional.

The 'for-each' commands applies the same formatting or commands to each element that matches the 'select' attribute. In Figure D.3 'for-each' is used to style each meeting the same way and each agenda item for a particular meeting the same way. Different templates can be written and called within a single XSLT file as well. Here, it is primarily shown for organization, but the ability to write a single template that may apply to many different XML files or tags within an XML file is a very useful feature. The result of this stylesheet is shown in Figure D.4.

This may appear overly verbose for the information it contains, but having this data in XML format gives us several advantages. First, writing an XSD schema for this file ensure that the minutes of each meeting are entered in the same format. Once we are confident that each meeting is entered in the correct format, XSLT stylesheets can be used to style this data. Now, for example, we can develop a web page that will display the information with the added benefits that the data in the XML file can be updated without changing the XSLT (or web page), and the web can be altered without changing the data stored in the XML.

A concrete example of this principle is WebNucleo's Solar Abundances Tool. Here, a user can upload their own solar abundance information and have it styled with WebNucleo's stylesheet. In addition, the XSLT calculates other relevant quantities for the user and the data can be sorted by any element in ascending or descending order[4] .

Using XML to organize one's data also makes it easy to share data with the Astrophysical community. Whereas you might have to explicitly describe the format of an ASCII data file to a colleague including units, dimensions, initial conditions, etc.; that information can all be contained in an XML file and checked with a XSD schema to ensure everything is properly formatted.

D.2 IDL: Interactive Data Language

ITT Visual Information Solutions, Interactive Data Language (IDL) is a commercial computer language frequently used by astronomers. IDL has many advantages that

[4] The Solar Abundances Tool is discussed in more detail in Chapter 3 and Appendix E.

```
<xsl:stylesheet version="1.0"
  xmlns:xsl="http://www.w3.org/1999/XSL/Transform"
>
  <xsl:template match="/">
    <html>
      <head><title>Minutes</title></head>
      <body>
        <table cellpadding="0">
          <tr bgcolor="#FFCC33" >
            <td width="50px"  />
            <td><h1><font color="#FFFFFF">Meeting Minutes</font></h1></td>
          </tr>
          <tr>
            <td />
            <td>
              <xsl:for-each select="//meeting">
                <xsl:sort select="date" order="descending" />
                <xsl:call-template name="one_meeting" />
              </xsl:for-each>
            </td>
          </tr>
        </table>
      </body>
    </html>
  </xsl:template>
  <xsl:template name="one_meeting">
    <h2><xsl:value-of select="date" /></h2>
    <table border="1">
      <xsl:for-each select="item">
      <tr>
        <xsl:choose>
          <xsl:when test="position() mod 2 = 0">
            <xsl:attribute name="bgcolor">#CCCCCC</xsl:attribute>
          </xsl:when>
        </xsl:choose>
        <td width="100px"><xsl:value-of select="presenter"/></td>
        <td width="200px"><xsl:value-of select="title" /></td>
      </tr>
      </xsl:for-each>
    </table>
  </xsl:template>
</xsl:stylesheet>
```

Figure D.3 This XSLT example will style the minutes XML file from Figure D.1. Here an HTML file is written that displays a list of the meetings and each agenda item for that meeting.

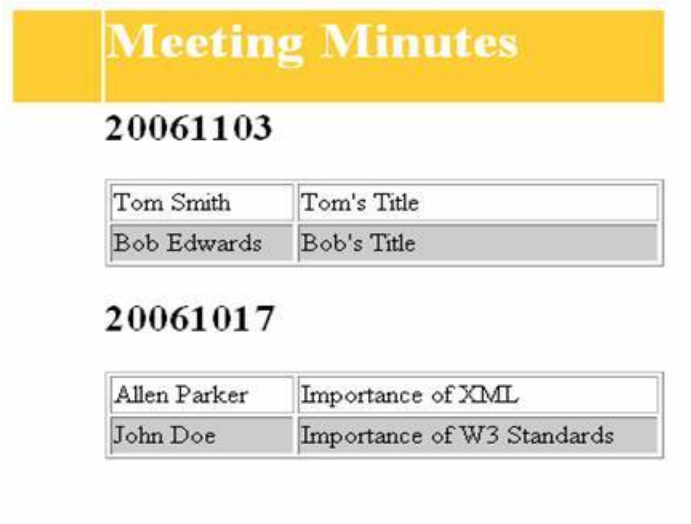

Figure D.4 Here, a very basic webpage has been made from the XML file and the XSL file.

are useful when developing tools for astronomy. First, IDL comes packaged with its own environment. This means IDL programs, functions or procedures are, in a sense, platform independent. This is important when sharing source amongst groups who use different platforms such as Windows, Linux, Solaris, MacOS, and others.

Also, IDL has a very modest learning curve when compared to other programming languages such as C or Fortran. Variable declarations and memory management are not the direct responsibility of the user, for example. Also, IDL has many convenient functions ideal for mathematical operations on data stored in arrays.

For more advanced applications, one can use IDL to style a widget based front end to make interacting with program more user friendly. Since IDL is a commercial language, it is not free software. This can often be a disadvantage but ITT provides the 'IDL Virtual Machine' for free which can run precompiled IDL procedures. Though there are some limitations on the Virtual Machine, it allows us to distribute some of our programs to the general public who do not have access to a full licensed version of IDL.

For web development, IDL On the Net, commonly referred to as ION, is available. Webnucleo uses ION as a convenient way to interact with IDL for many of our Online Tools.

D.3 HDF: Hierarchical Data Format

For many of Webnucleo's applications we use XML because it is easily readable and can easily place data in a logical hierarchy. However, when data sets become large or processing speed is more important, XML is not the most efficient format to store the data. For example, Webnucleo's 1d Stellar Ejecta Module can require very large data sets, which introduces many different computational problems that must be addressed. Some of the concerns include: human readability, file size, efficiency of input and output, and multi-user or processor collisions. HDF5 is the latest version of a Hierarchical Data Format developed by the National Center for Super Applications (NCSA) that addresses these concerns.

HDF5 files are much more compact then XML files containing comparable data. However, HDF5 files are binary files that cannot be opened by a normal texteditor. In order to make HDF5 files more easily readable, NCSA developed HDFview. HDFview opens an HDF5 file and displays the data in a hierarchy similar to what is done by XML readers that are available. Groups can be created within an HDF5 file that contains several datasets or other groups. Figure D.5 is an example of what one sees in HDFview. Groups can be expanded and contracted for more easy readability. Also, HDFView has a built in feature to make simple plots. This can often be useful when previewing data before running it through a potentially lengthy computation.

When dealing with very large datasets, the compression of the storage format can be very important. XML documents have verbose tags around each individual datum, but an HDF5 file stores data in 'chunks' that greatly reduces the amount of space needed to store the data. The size of the data file can affect the efficiency of a program tremendously. A one hundred megabyte XML file might result in an HDF5 file twenty megabytes, for example. In addition, before extracting the data from the files, they have to be loaded into memory. Memory allocation is often a source of inefficiency, and the HDF5 file starts with a large advantage over XML. Also, for an HDF5 file, a single 'chunk' of data can be extracted from the file without having to load the entire document. Thus for applications where small

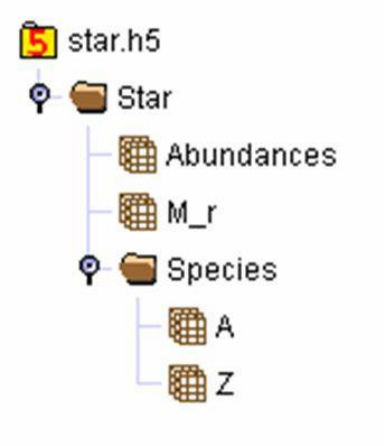

Figure D.5 Shown here is a screenshot of an HDF5 file used in Webnucleo's 1d Stellar Ejecta Module. The various groups allow the data to be organized hierarchically for easy readability.

data subsets are needed from larger datasets HDF5 reduces computational overhead and will result in a more efficient program.

This 'chunking' mechanism is also useful for parallel processing codes. That way, one processor can be reading from one chunk of data and modifying, while another chunk of data is being processed simultaneously by another processor.

Appendix E

Solar Abundances Tool: WebNucleo Technical Report

This report describes the XML schema and the calculations performed by the Solar Abundances Tool. The tool itself and tutorials explaining its use can be found at:

http://nucleo.ces.clemson.edu/home/online_tools/solar_abundances/0.1

E.1 Upload Table

The first panel of the Solar Abundances Tool is the 'Upload Table' panel. This panel gives the user the option of using the default table provided or uploading their own. The table used by the Solar Abundances Tool must be an XML file in the appropriate format. In the tutorials, users are encouraged to download the distribution and modify an existing XML. This ensures all namespace information is of the proper format. For more detail on the format of the XML file, an XSD schema is provided at ./xsd_pub/solar_abundance_distribution.xsd .

When the XML file is loaded, the calculations for the tool are performed using an XSL stylesheet and an IDL routine. The XSL stylesheet calculates the neutron number (N) from the mass number (A) and the atomic number (Z) according to the simple relationship:

$$N = A - Z \tag{E.1}$$

The XSL stylesheet also calculates the fractional abundances. These are calculated from the abundances in the XML file. This calculation takes the individual abundance over the sum of all of the abundances as shown in Equation E.2.

$$\text{Fractional Abundance}_i = \frac{\text{Abundance}_i}{\sum_{j=1}^{N} \text{Abundance}_j} \tag{E.2}$$

The mass fraction is calculated similarly where the mass of an individual species is calculated by multiplying its abundance by its atomic number, A. The mass fraction of a species can

then be calculated by dividing the individual mass by the sum of all the masses in the table (Equation E.3).

$$\text{Mass Fraction}_i = \frac{\text{Abundance}_i * A_i}{\sum_{j=1}^{N} \text{Abundances}_j * A_j} \tag{E.3}$$

It should be noted that in order to use scientific notation, which is not supported by default in XSLT 1.0, webnucleo_scientific.xsl is used. A copy of this file is present in the 0.1 release of the Solar Abundances Tool, but will be moved to the wn_xml_utils module in future releases.

Lastly, the grouped abundances are calculated by grouping the abundances together by a common Z, N, or A. These groups are referred to as Y(Z), Y(N), and Y(A) respectively. This calculation is done in an IDL routine, elemental_abundances.pro, which is available in the downloadable distribution. For this tool, a temporary bat file is written that contains the IDL script to be executed. This bat file is then executed on the server with IDL 6.3. This is different than some of the other Webnucleo tools that use the ION script with an older version of IDL.

E.2 Sort Data

The 'Sort Data' panel of the Solar Abundances Tool takes the isotopic abundances from the generated XML and sorts it according to the selection of the user. The sorted table is generated using an XSL stylesheet that accepts a parameter corresponding to the users sort selection and a parameter that indicates whether to sort in ascending or descending order. A 'Rank' column is also added to the styled data. This is meant for the convenience of the user. If one uploads a modified set of isotopic abundances, a small change in abundance may have a noticeable affect to a particular isotope's rank. For example, ^{18}O in the table from the default compilation of Anders and Grevesse [1989] is the twenty-second most abundant species, whereas it is the twenty-fifth compilation of Lodders [2003].

The stylesheet also calls webnucleo_strings.xsl, which is used to style the display names for the different species. For example, an entry with Z=14 and A = 28 would be displayed as ^{28}Si. This feature was added to help the readability of the displayed data.

Like webnucleo_scientific.xsl, webnucleo_strings.xsl will reside in the wn_xml_utils module for future releases.

E.3 Plot Abundances

The Plot Abundances panel refers to the elemental abundances. Here, the variables Y(Z), Y(N), and Y(A) can be plotted as functions of Z, N, and A respectively. For these plots the logarithmic option should be enabled for the y-axis.

The plots are generated using Webnucleo's Plot Tool. This tool standardizes the plots generated in any of Webnucleo's Online Tools, and the user's interaction with them. The Plot Tool calls IDL procedures that create a PNG image to be styled into the webpage.

Because plots like Y(Z) versus N are meaningless, the user only needs to select the 'plot on x-axis' field and the 'plot on y-axis' field is selected automatically. This is done using a series of Java-script functions that takes the selected value for the x-axis and forces the selection of the y-axis.

For example, the example below hides the Z element from the y drop menu. For the 'Plot Abundances' panel, the Z, A, and N elements are hidden from the y-axis drop menu.

```
document.getElementById(
  'plot_tool.ys.option.y_axis.n_nz'
).style.display='none';
```

To rewrite the title of the Y(Z) in the x-axis drop with a null string the example below is used. This is done because, traditionally, only Z, A, or N will be placed on the x-axis. So the Y(Z), Y(N), and Y(A) options are removed from the x-axis.

```
rewrite_simple_element_content(
  document.getElementById(
    'plot_tool.ys.option.x_axis.y_a_nz'
  ),''
);
```

In order to determine which item the user has selected from the x-axis drop menu, the the command below is used.

```
var i_x_selindex=document.getElementById('plot_tool.ys.xaxis').
  selectedIndex;
```

This last example shows how to check the user's selection and force the correct parameter to be shown in the y-axis drop.

```
if(document.getElementById('plot_tool.ys.xaxis').
  options[i_x_selindex].text=='Z'
){
  document.getElementById('plot_tool.ys.yaxis').
    options[0].value='y_z_nz';
  document.getElementById('plot_tool.ys.yaxis').
    options[0].text='Y(Z)';
}
```

It is worth noting that the current version of Internet Explorer, at the time of this release, is unable to hide irrelevant elements in the drop down menu. So, instead, each element of the drop down that is not needed is replaced with a null string.

E.4 Table of Abundances

The Table of Abundances panel generates tables containing the Z, N, A, Y(Z), Y(N), and Y(A) data. Since Z, N, and A are all integers, the table is made with a variable called Index. An Index of 3, for example, will refer to Z=3 for the Y(Z) column, A=3 for the Y(A) column, and N=3 for the Y(N) column.

The tables are generated using Webnucleo's 'Table Tool'. Again, this is done to standardize the tables generated for all Webnucleo tools and the user interface with them. The user may choose to generate an HTML table or an ASCII table. XSL stylesheets style the data based on the user's selection.

E.5 Plot All

The Plot All panel generates plots with any of the following variables; Z, N, A, Abundance, Mass Fraction, and Fractional Abundance. Since all of these values refer to individual species, plots may have several values for a particular Z, N, or A. Users are encouraged to make plots with the data points shown, and the line connecting them turned off. Again, for numbers on this scale, users will want to enable logarithmic plotting for the y-axis.

E.6 Full Table

The Full Table panel also uses the variables Z, N, A, Abundance, Fractional Abundance, and Mass Fraction. The tables generated on this panel may contain much of the same information as the Sort Table panel. The user may select to limit the entries in the table in order to display only the information relevant for them.

Appendix F

Newton Tool: WebNucleo Technical Report

The following is a brief explanation of the IDL code at the base of the Newton Tool. This report describes the algorithm used and the calculations performed in IDL and a bit about its applications and limits. The tool itself and tutorials explaining its use can be found at:

http://nucleo.ces.clemson.edu/home/online_tools/newton/0.2 .

F.1 Fourth-Order Runge-Kutta

At the root of the IDL procedure, newton_nd.pro, is the fourth order Runge-Kutta function, rk4, which is native to IDL. This function accepts an array, y, of n variables and n first derivatives of those variables in the form:

$$\begin{bmatrix} q_1 & q_2 & \cdots & q_n & \dot{q}_1 & \dot{q}_2 & \cdots & \dot{q}_n \end{bmatrix} \tag{F.1}$$

The rk4 function then propagates this array forward one small step in the dependent coordinate using a set of n differential equations supplied by the user. Since the differential equations supplied are second order, the Newton Tool breaks each equation into two first order differential equations. Time is the dependent variable for this tool. So, the first order differential equations are:

$$\frac{dq_i}{dt} = \dot{q}_i \tag{F.2}$$

$$\frac{d\dot{q}_i}{dt} = \ddot{q}_i \tag{F.3}$$

For the Newton Tool, the coordinates are the variables x, y, z, and the first derivatives are with respect to time. These variables are named after the classic Cartesian variables but can represent any generalized coordinates.

F.2 Adaptive Time Step

In the Newton Tool's main loop, another IDL function is called that can change the step size. This is done using the equation for the fifth order truncation error:

$$(\Delta t)_0 = (\Delta t)_1 \left| \frac{(\Delta x)_0}{(\Delta x)_1} \right|^{\frac{1}{2}} \tag{F.4}$$

The IDL function, stepfunc.pro, uses this equation to scale the step size for the next iteration. In Equation *F*.4, $(\Delta x)_1$ represents the difference between the change in the variable made with one time step of size $(\Delta t)_1$ and two iterations with a step size of $(\Delta t)_1/2$ The variable $(\Delta x)_0$ is the desired accuracy of the iterations. The ratio of these two differences scales the next time step. This scaling prevents the code from going through too many iterations for a simple problem, or not accurately propagating the motion of a system that requires high accuracy.

F.3 Online Tool (Front End)

The online Newton Tool is a front end written around the IDL procedure. The tool obtains the necessary initial parameters from the user to be entered into the IDL function. The parameters that are needed are the differential equations (accelerations), initial conditions, and the parameter for the adaptive step.

In order to be user friendly, the strings are taken in terms of Cartesian variables, their associated velocities, and time. These, more explicitly, are; x, y, z, vx, vy, vz, and t. These equations are then checked with a function called 'check_string' that replaces these variables with the variable names as used in the newton_nd procedure shown in Equation *F*.1.

If the necessary information has been entered, the 'Calculate' button located on the 'Initial Conditions' Panel calls the IDL procedure to propagate the system. The resulting data is written to a temporary file which can then be read by the 'Plot Tool' and 'Table Tool'. The 'Plot Tool' allows the user to make a two dimensional plot of any of the parameters propagated through the code. The 'Table Tool' lets the user make a table of the parameters in either an ASCII or html format.

F.4 Limitations

The current limitations of the Newton Module mostly involve scaling problems. The success of a given simulation is highly dependent upon how accurate each time step is. Equations or initial conditions that produce numbers very large of very small may cause problems in the rk4 function called. To address this issue, the Tool's Tutorials contain tips on assuring appropriately scaled numbers and equations are entered.

Another limitation is that, because the tool is written for a general set of equations, it does not check to make sure the equations are not evaluated with a zero in the denominator. This may lead to the Newton Tool crashing and failing to return the motion because of undefined point it tried to evaluate. The Tool's Tutorials contains information regarding this limitation and suggestions to user with how to deal with it.

Lastly, the user may find computation time to be a limitation as well. Because the calculations are performed on the webnucleo server, an individual calculation is limited to run within a time interval of 3 minutes.

If more lengthy computations are required, the IDL source has been made available online under the Tool's Technical Resources. The interested user may download this source code to run longer calculations and to modify the source for particular applications.

BIBLIOGRAPHY

Adams, D. C. 2006. Libnucnet, wn_matrix, and Their Applications. M.S. thesis, Clemson University.

Anders, E. and Ebihara, M. 1982. Solar-System Abundances of the Elements: A New Table. *Meteoritics 17*, 180–+.

Anders, E. and Grevesse, N. 1989. Abundances of the elements - Meteoritic and solar. *Geochim. Cosmochim. Acta 53*, 197–214.

Arnett, D. 1996. *Supernovae and nucleosynthesis. an investigation of the history of matter, from the Big Bang to the present.* Princeton series in astrophysics, Princeton, NJ: Princeton University Press, —c1996.

Asplund, M., Grevesse, N., and Sauval, A. J. 2005. The Solar Chemical Composition. In *ASP Conf. Ser. 336: Cosmic Abundances as Records of Stellar Evolution and Nucleosynthesis*, T. G. Barnes, III and F. N. Bash, Eds. 25–+.

Cameron, A. G. W. and Truran, J. W. 1977. The supernova trigger for formation of the solar system. *Icarus 30*, 447–461.

Carroll, B. W. and Ostlie, D. A. 1995. An introduction to modern astrophysics.

Darling, D. 2006. The Encyclopedia of Asrtrobiology Astronomy and Spaceflight.

Faure, G. 1986. *Principles of Isotope Geology*, 2nd ed. Number 28 July 2006. John Wiley & Sons, Inc., New York.

Goldberg, L., Muller, E. A., and Aller, L. H. 1960. The Abundances of the Elements in the Solar Atmosphere. *Astrophys. J. Suppl. 5*, 1–+.

Grevesse, N. and Sauval, A. J. 1998. Standard Solar Composition. *Space Science Reviews 85*, 161–174.

Kerridge, J. F. and Matthews, M. S. 1988. *Meteorites and the early solar system.* Meteorites and the Early Solar System.

Lodders, K. 2003. Solar System Abundances and Condensation Temperatures of the Elements. *Astrophys. J. 591*, 1220–1247.

Meyer, B. S. 1997. Supernova Nucleosynthesis. In *American Institute of Physics Conference Series*, T. J. Bernatowicz and E. Zinner, Eds. 155–+.

Meyer, B. S. 2005. Synthesis of Short-lived Radioactivities in a Massive Star. In *ASP Conf. Ser. 341: Chondrites and the Protoplanetary Disk*, A. N. Krot, E. R. D. Scott, and B. Reipurth, Eds. 515–+.

Meyer, B. S. and Clayton, D. D. 2000. Short-Lived Radioactivities and the Birth of the sun. *Space Science Reviews 92*, 133–152.

NASA. 1991. Information Summaries: Our Solar System at a Glance.

Podosek, F. A. 2005. Overview of Origin of Short-lived Radionuclides, Chronology of Refractory Inclusions and Chondrules. In *ASP Conf. Ser. 341: Chondrites and the Protoplanetary Disk*, A. N. Krot, E. R. D. Scott, and B. Reipurth, Eds. 471–+.

Richard, O., Dziembowski, W. A., Sienkiewicz, R., and Goode, P. R. 1998. Precise Determination of the Solar Helium Abundance by Helioseismology. In *Structure and Dynamics of the Interior of the Sun and Sun-like Stars SOHO 6/GONG 98 Workshop Abstract, June 1-4, 1998, Boston, Massachusetts, p. 517*, S. Korzennik, Ed. 517–+.

Russell, H. N. 1929. On the Composition of the Sun's Atmosphere. *Astrophys. J. 70*, 11–+.

Scott, E. R. D. and Krot, A. N. 2005. Chondritic Meteorites and the High-Temperature Nebular Origins of Their Components. In *ASP Conf. Ser. 341: Chondrites and the Protoplanetary Disk*, A. N. Krot, E. R. D. Scott, and B. Reipurth, Eds. 15–+.

Unsöld, A. 1948. Quantitative Analyse des Spektrums einer eruptiven Protuberanz. Mit 2 Textabbldungen. *Zeitschrift fur Astrophysik 24*, 22–+.